A review of operational systems for tropical forest monitoring from satellite remote sensing: *A technical description and product comparison for the Congo Basin*

This document is the first complementary study conducted by the UCLouvain for the Obsevatoire des Forêts d'Afrique Centrale (OFAC) as part of the RIOFAC 2 project.

Authors

Thibauld Collet, Baptiste Delhez, Benjamin Goffart, Thomas De Maet, Pierre Defourny

UCLouvain

November 2023

Résumé

Cette étude, réalisée par l'UCLouvain dans le cadre du projet RIOFAC 2 soutenu par la Commission européenne, présente une analyse comparative approfondie de plusieurs systèmes opérationnels pour la surveillance des forêts tropicales à partir de la télédétection par satellite. Cette étude offre une description technique et une comparaison des produits pour la forêt dense humide du Bassin du Congo comme travail préliminaire pour la consolidation de la détection de la déforestation et de la dégradation. La revue de la littérature a permis d'identifier six systèmes opérationnels de détection de la déforestation par satellite qui se distinguent par leur couverture spatiale et temporelle pertinente, leur méthodologie innovante ou la robustesse de leurs détections. Les différentes parties prenantes, les performances des systèmes et les paradigmes actuels ont également été décrits et discutés afin d'obtenir une vue d'ensemble complète de l'état de l'art dans le domaine de la surveillance opérationnelle des forêts par satellite.

Parmi les systèmes décrits dans ce document, deux d'entre eux se distinguent par leur capacité à fournir des estimations à long terme, exhaustives et opérationnelles de la déforestation aux niveaux régional, national et local : Tropical Moist Forest (TMF) développé par le Joint Research Center et Global Forest Change (GFC) produit par l'Université du Maryland. Ces deux ensembles de données constituent la source la plus populaire pour le suivi de la déforestation et utilisent à peu près les mêmes archives Landsat dans leurs modèles de détection de la déforestation.

Malgré des objectifs et des données satellitaires d'entrée similaires, une analyse comparative approfondie, à la fois qualitative et quantitative, met en évidence des divergences majeures entre les systèmes de détection qui vont au-delà d'une simple différence de définition et de sensibilité entre deux modèles de détection. L'analyse méthodologique et comparative met en évidence le fait que TMF offre une détection presque exhaustive des perturbations forestières au prix d'un nombre élevé de fausses détections, alors que GFC tend à produire des détections plus fiables au prix d'un nombre plus élevé d'omissions. Les détections de GFC sont principalement situées à l'intérieur des forêts à canopée fermée et détectent donc moins de changements dans les forêts plus ouvertes ou secondaires. Les détections TMF sont situées dans tous les couverts forestiers de la zone dense et humide, y compris les couverts très dégradés.

Le système de surveillance des forêts GFC rapporte une étendue de perturbation forestière de 7,44 Mha tandis que le système TMF a détecté 28,53 Mha en considérant leurs masques forestiers respectifs. En utilisant uniquement le masque forestier le plus restrictif pour les deux systèmes, l'analyse, au niveau des pixels, indique une correspondance spatiale de 53 % pour la détection des perturbations forestières entre 2001 et 2021 pour l'ensemble du Bassin du Congo. Les cartes régionales et nationales mettent en évidence les convergences et les divergences entre les deux systèmes à la résolution native de 30 m, décrivant également les différentes sensibilités des systèmes en fonction des types d'occupation du sol.

Il est primordial que les résultats avancés n'invalident pas les systèmes opérationnels actuels. Certaines des conclusions sont la conséquence des choix méthodologiques et des paradigmes utilisés, qui sont présentés de manière transparente par les différents systèmes. Néanmoins, cette analyse comparative complète recommande de faire preuve de prudence lors de l'utilisation de ces données, en reconnaissant que l'utilisation de l'une ou l'autre source de données conduit à des résultats locaux et régionaux différents. La compréhension des forces et des faiblesses de chaque système permettra une intégration prudente et adaptée aux besoins et appelle à un système consolidé de déforestation harmonisé pour les pays de la COMIFAC.

Summary

This study completed by the UCLouvain in the framework of the RIOFAC 2 project supported by the European Commission, presents a in-depth comparative analysis of several operational systems for tropical moist forest monitoring from satellite remote sensing. This study offers a technical description and product comparison for the Congo Basin moist forest as a preliminary work for consolidation the detection of deforestation and degradation. The literature review has identified six operational satellite deforestation detection systems that stand out for their relevant spatial and temporal coverage, their innovative methodology or the robustness of their detections. The various stakeholders, the performance of the systems and the current paradigms were also described and discussed in order to have a complete state-of-the art overview in the field of operational satellite-based forest monitoring.

Among the systems described in this document, two of them stand out for their capacity to provide long term, exhaustive, and operational estimates of deforestation at regional, national, and local levels: *Tropical Moist Forest* (TMF) developed by the Joint Research Centre and *Global Forest Change* (GFC) produced by the University of Maryland. Both datasets are the most popular source for deforestation monitoring and use roughly the same Landsat archives in their deforestation detection models.

Despite having similar objectives and input satellite data, an in-depth comparative analysis, both qualitative and quantitative, highlights major discrepancies between system detection that go beyond a simple difference in definition and sensitivity between two detection models. Methodological and comparative analysis highlight the fact that TMF offers an almost exhaustive forest disturbances at the cost of high false detection as GFC tends to produce more trustworthy detections at the cost of higher omission. GFC detections are mostly located inside closed canopy forests and so detect less changes in more open or secondary forests. TMF detections are located in all forest canopies within the dense and humid zone, including highly degraded canopies.

The GFC forest monitoring system reports a forest disturbance extent of 7,44 Mha while the TMF system detected 28,53 Mha when considering their respective forest masks. Using only the most restrictive forest mask for both systems, the pixel-based wall-to-wall analysis indicates a spatial correspondence of 59 % for the forest disturbance detection between 2001 and 2021 for the whole Congo Basin. Regional and national maps highlight the convergence and discrepancies between both systems at the native 30 m resolution, depicting also different system sensitivities according to the land surface.

It is of paramount importance that these advanced results do not invalidate the current operational systems. Some of these conclusions are a consequence of the methodological choices and paradigms used, which are transparently presented by the different systems. Nevertheless, this comprehensive comparative analysis does recommend exercising caution when using this data, acknowledging that utilizing one or the other source of data leads to different local and regional results. Understanding the strengths and weaknesses of each system will enable careful fit for purpose integration and calls for a harmonized consolidated deforestation system for the COMIFAC countries.

Symbols and acronyms

ALT	Adaptative Linear Thresholding
API	Application Programming Interface
ARD	Analysis Ready Data (Landsat)
BDI	Republic of Burundi
CAFI	Central African Forest Initiative
CAR	Central African Republic
CESBIO	Centre d'Etudes Spatiales de la Biosphère
CMR	Republic of Cameroon
CNES	Centre National d'Etudes Spatiales
CNN	Convolutional Neural Network
COMIFAC	Commission des Forêts d'Afrique Centrale
DEF	Deforestation data from the Tropical Moist Forest dataset
DEG	Degradation data from the Tropical Moist Forest dataset
DETER-R	DETERring Deforestation in the Amazon using Radar images
DRC	Democratic Republic of the Congo
ETM+	Enhanced Thematic Mapper Plus
FD	Forest Disturbance
GAB	Gabonese Republic
GEE	Google Earth Engine
GFC	Global Forest Change dataset
GFW	Global Forest Watch
GLAD	Global Analysis and Discovery
GLADa	Global Analysis and Discovery alert system
GNQ	Republic of Equatorial Guinea
GRD	Ground Range Detected
HSV	Hue, Saturation, Value
IBGE	Brazilian Institute from Geography and Statistics
INPE	Brazilian National Institute for Space Research
MODIS	Moderate Resolution Imaging Spectroradiometer
NBR	Normalized Burned Ration
NDVI	Normalized Difference Vegetation Index
NDWI	Normalized Difference Water Index
NIR	Near infrared
NRT	Near real Time

OFAC	Observatoire des Forêts d'Afrique Centrale
OLI	Operational Land Imager (Landsat)
OTB	Orfeo Toolbox (OTB)
PEPs	Sentinel Product Exploitation Platform
PRODES	Brazilian Amazon Rainforest Monitoring Program by Satellite
RADD	Radar for Detecting Deforestation
RCR	Radar Change Ration (RCR)
RIOFAC	Renforcement et Institutionnalisation de l'Observatoire des Forêts d'Afrique Centrale
ROC	Republic of Congo
RWD	Republic of Rwanda
S1	Sentinel 1
S2	Sentinel 2
SAR - (X, C)	Synthetic Aperture Radar in X or C band
SCO	Space for Climate Observatory
SRTM	Shuttle Radar Topography Mission (SRTM)
SWIR2	Short-Wave Infrared
TIR	Thermal Infrared
TIRS	Thermal Infrared Sensor (Landsat)
TMF	Tropical Moist Forest (dataset from the Joint Research Center)
TROPISCO	Tropical Space for Climate Observatory
UAV LIDAR	Unmanned Aerial Vehicles Light Detection and Ranging
UMD	University of Maryland
USGS	United States Geological Survey
VH	Vertical/Horizontal
VV	Vertical/Vertical

Table of contents

List of figures

List of tables

1. Introduction

1.1 Scope

This study was conducted by the UCLouvain as part of the RIOFAC 2 project. It presents a critical comparative analysis of various operational systems for tropical moist forest monitoring based on satellite remote sensing. This study offers a technical description and products comparison for the Congo Basin moist forest as a preliminary work for the consolidation of deforestation and degradation detections of the various datasets.

1.2 Background and justification

As satellite data archives grew longer, change detection methods became more refined and the need for more information about forest dynamics at global scale became more pressing. In this context, a series of satellite-based forest disturbance detection systems have been developed. These systems were often created for specific needs and purposes, making their combination complex and hazardous. Initiatives such as Global Forest Watch (GFW) have set out to bring all this information together and make it available to most people. Those data are now being used by many stakeholders in a wide array of applications sometimes without critical consideration. The aim of this document is therefore to provide an in-depth analysis of the various forest disturbance detection systems in the dense rainforests of Central Africa, with an in-depth analysis of the two most popular systems for long-term forest monitoring: the Global Forest Change (GFC) and the Tropical Moist Forest (TMF) datasets.

1.3 Structure of the document

This document is divided in two sections. The first section offers a benchmarking of four near-real-time and two annual state-of-the-art currently operational forest disturbance monitoring systems. Each system is described regarding six sections, beginning with a short presentation of the main claims, aims and origins. As important terms like *forest disturbance* or *forest extent* differs according to each system, brief explanations are given. Then the input data origins/pre-processing and the complete summarized methodology are presented. Finally, the system validation is summarized and confronted to existing independent evaluations. All open-source data (input, output, and source code) are referenced throughout the document.

The second section is dedicated to a more in-depth comparison of GFC and TMF datasets for the Congo Bassin long term forest monitoring. This critical analysis will provide the strengths and weaknesses of both systems as well as qualitative and quantitative assessments about their relative performances and specificities for the Congo Bassin particular characteristics (i.e. cloud free data availabilities and forest dynamics).

2. Technical review of the operational systems

2.1 GFC (Global Forest Change): -Annual percent tree cover and forest change datasets-

Presentation

Global Forest Change (GFC) is global mapping dataset aiming to provide consistent and spatially explicit annual quantitative information's about tree cover loss and gains. It was developed in 2013 and annually updated by Global Analysis and Discovery laboratory (GLAD) of the University of Maryland (UMD). This product is currently freely accessible as an "Ground occupation" layer on the GFW online platform[1]. The system is running on an open-source Google Earth Engine (GEE) online application[2].

Key concept definition

The GFC product (Hansen *et al*., 2013a) aims to map forest as **tree cover**. As such, **forest** is defined as a 30x30m Landsat pixel having at least a small detectable (by Landsat sensor) vegetation cover higher than 5m (trees). **Forest disturbance** (FD) is defined as a stand-replacement/complete removal of tree cover (tree cover ~0%). **Forest gain** is defined as the establishment of a tree cover on a previously non-forested area.

Input data

GFC input data varies according to the product version and to the year of interest. While previous version only uses growing season Landsat 7 Enhanced Thematic Mapper Plus (ETM+) data, the latest version adds Landsat 8 Operational Land Imager (OLI) data to the forest change detection for the period 2013-2021. Data followed generic prepossessing steps including image resampling, conversion from digital values to top of atmosphere reflectance or image normalization.

The forest change detection model relies on metrics computed using time series. Those metrics include "*minimal, maximal and selected percentile reflectance values, mean reflectance values for observations between selected percentiles and slope of linear regression of band reflectance value versus image date"* (Hansen *et al*., 2013b). The precise procedure to compute those metrics is described in the "phenological metrics" section of GLAD web site[3].

Methodology

In order to measure forest change, it is necessary to define a reference forest extent. As such, the first step of GFC mapping is to produce an annual tree cover map referencing the percent tree cover density of each pixel. It is produced by a decision tree trained with samples labelled using Landsat image visual interpretation and characterized by time series metrics. This map was produced in 2000 and 2010 and used extensively since 2013 as forest cover reference in many studies.

The same methodology is used to detect forest loss and gain on an annual basis. First, full time series derived metrics are computed for a period of at least a four-year period including the year of interest. Then, machine learning principles, training dataset acquired using visual interpretation and the time series metrics are used in order to train a bagged decision tree.

This procedure allows the model to detect whether or not a forest change happen during the time series, but it do not output the actual date of this change. To find this date, the annual maximum and minimum decline in NDVI is computed for each year of the time series. The year with the highest decline is define

[1] (https://global forestwatch.org)
[2] (https://glad.earthengine.app/view/global-forest-change).
[3] (https://glad.umd.edu/ard/phenoa)

as the forest loss date for pixels that are classified as forest loss. The year with the lowest decline is define as the forest gain date for pixels that are classified as forest gain.

GFC products are regularly updated by GLAD laboratory in order to take advantages of new data prepossessing method, new data availability and new training samples collection. The latest versions are available at the Google hosted GLAD Application Programming Interface[4] (API).

The latest version GFC source code is available on the GEE developer's platform[5].

Validation and Results

Validation samples are collected using visual interpretation of Landsat time series, Modis time series and GEE imagery. In tropical forest, producer's accuracy for forest loss and gain are respectively 0.83 and 0.46 while User's accuracy for forest loss and gain are respectively 0.87 and 0.82. Those results shows that forest gain might be underestimate in tropical area. It is worth noting that there is a high uncertainty in the validation estimates (Hansen *et al*., 2013b) for tropical regions.

Evaluation

Since its release in 2013, GFC products and methodology were used as forest extent reference in an uncountable number of applications. In fact, it is fairly simple and straightforward detection procedure as well as its reference percent tree cover map allow users to extract initial forest extents in regards with their own forest definition (in term of percent coverage, usually ≥50% tree cover).

However, early criticism by Tropek *et al* (2014) regarding GFC forest definition and its impact on forest change monitoring were given. Those critics highlight the fact that adding tree plantations to the forest map and including low tree cover density in the forest definition might be misleading for most application and lead to forest extent overestimation in regards with commonly established forest definition. Those critics, recognized by GFC developers, were mitigated by the fact that GFC never aimed to monitor forest as a land use, but as a percent tree cover Hansen *et al* (2015).

Sannier et al (2015) exposed the issues encountered when applying a global product at a local scale (Gabon). They highlight the requirement to apply specific percent tree cover calibration for each area of interest in order to obtain usable forest extent. They also noticed that GFC overestimates forest loss area. In contrary, other studies show that GFC tends to underestimate deforestation rates and fail to detect forest gain after 2012 (Milodowski et al.,2017).

Given the relative oldness and its extensive use as a reference forest extents generator, the accuracy of GFC products have been assessed like no other forest monitoring systems. In general, studies highlight the inconsistency of GFC products performances in local tropical applications (Kinnebrew *et al*., 2022) reflecting the importance of wisely using global product at local scale.

Hansen, M. C.; Potapov, P. V.; Moore, R.; Hancher, M.; Turubanova, S. A.; Tyukavina, A.; Thau, D.; Stehman, S. V.; Goetz, S. J.; Loveland, T. R.; Kommareddy, A.; Egorov, A.; Chini, L.; Justice, C. O.; Townshend J. R. G. ***Supplementary Materials for High-Resolution Global Maps of 21st-Century Forest Cover Change Science.*** 342, 850 (2013b); https://doi.org/10.1126/science.1244693

Hansen, M. C.; Potapov, P. V.; Moore, R.; Hancher, M.; Turubanova, S. A.; Tyukavina, A.; Thau, D.; Stehman, S. V.; Goetz, S. J.; Loveland, T. R.; Kommareddy, A.; Egorov, A.; Chini,

[4] (https://storage.googleapis.com/earthenginepartners-hansen/GFC-2021-v1.9/download.html)
[5] (https://developers.google.com/earth-engine/tutorials/tutorial_forest_03)

L.; Justice, C. O.; Townshend J. R. G. ***High-Resolution Global Maps of 21st-Century Forest Cover Change.*** 342, 850 (2013b); https://doi.org/10.1126/science.1244693

Hansen, M.; Potapov, P.; Margono, B.; Stehman, S.; Turubanova, S.; Tyukavina, A. ***Response to Comment on "High-resolution global maps of 21st-century forest cover change"***. Science 344, 981-e (2015); https://www.researchgate.net/publication/262734548

Kinnebrew, E.; Ochoa-Brito, JI.; French, M.; Mills-Novoa, M.; Shoffner, E.; Siegel K. ***Biases and limitations of Global Forest Change and author-generated land cover maps in detecting deforestation in the Amazon***. PLOS ONE 17(7): e0268970 (2022); https://doi.org/10.1371/journal.pone.0268970

Milodowski1, D T.; Mitchard E. T. A.; Williams M. ***Forest loss maps from regional satellite monitoring systematically underestimate deforestation in two rapidly changing parts of the Amazon.*** Environ. Res. Lett. 12 094003; https://doi.org/10.1088/1748-9326/aa7e1e

Sannier, C.; McRoberts, R; E.; Fichet, L. ***Suitability of Global Forest Change data to report forest cover estimates at national level in Gabon***. Remote Sensing of Environment, Volume 173, 2016, Pages 326-338, ISSN 0034-4257; https://doi.org/10.1016/j.rse.2015.10.032

Tropek, R.; Sedláček, O.; Beck, J.; Keil, P.; Musilová, Z.; Šímová, I.; Storch, D. ***Comment on "High-resolution global maps of 21st-century forest cover change"***. Science 344, 981 (2014); https://www.sciencemag.org/content/344/6187/981-d

2.2 TMF (Tropical Moist Forest) dataset

Presentation

TMF datasets are pan-tropical 30 m spatial resolution mapping products aiming to provide long-term period forest change monitoring. This dataset was developed in 2021 by the European Commission's Joint Research Centre (JRC) and is expected to be annually updated. The expert system is running on GEE online platform. All TMF products can be visualized and downloaded on the TMF explorer online application[6].

Key concept definition

Undisturbed moist forest is defined as a 0.09 ha area of closed dense semi-evergreen or evergreen forest that did not experience forest disturbance (FD) events during the whole Landsat dataset (1990-2021). A **FD** can be either **deforestation** or **degradation**. A deforestation refers to a long-term change (≥2.5 years) in land cover (from forest to non-forest land) when degradation refers to a temporary disturbance (≤2.5 years) in a forest remaining forested after the FD event such as selective logging, fires, and unusual weather events (hurricanes, droughts, blowdown). An area can thus be classified as degradation and then changed into deforestation if the tree cover loss persists.

Input data

TMF model uses the whole Landsat 4,5,7 (ETM+) and 8 (OLI) 30 years long archive. Despite this long time period, Vancutsem *et al*. (2021) highlight the spatial and temporal unevenness in the amount of valid data in Central Africa, especially in the Gulf of Guinea region where less than 50 valid observations per pixel are available for the whole Landsat archive. However, with the launch of Landsat 7 and 8, the amount of valid observation increases significantly. Still, in average Central Africa region is less covered by valid optical data than the rest of tropical areas.

No details are given for potential pre-processing; however, it can be assumed that generic optical data pre-processing are applied in addition to GEE-based pre-processing. Missing spectral band values and/or artefacts are removed from the dataset.

Methodology

TMF products are created using an expert system taking the form of a procedural sequential decision tree. The rules of this decision tree needed big data exploration, visual analysis, and evidential reasoning in order to be calibrated. The creation of annual change maps followed tree main steps.

First, a multidimensional spectral library is computed in order to characterize the spectral signature of each class. This library contains 38.326 babelized single-date sample points located in a multidimensional space where each dimension represents a computed metric. Those metrics are HSV (hue, saturation, value), transformed NIR (near infrared), SWIR2 (short-wave infrared) and Red spectral bands, Normalized Difference Water Index (NDWI) and thermal infrared (TIR) bands. Cluster hulls multidimensional equations were computed using the Pekel *et al*. (2016) visual analysis interactive tool. Those equations are then used to classify all available single-date pixels from the 30-year Landsat archive. The resulting **moist/non-moist forest map** will be used as the reference extent for further transition analysis. In order to perform relevant transition analysis, for a given pixel, the reference date is set only if a sufficient amount of valid observation is following (4 years with at least 3 valid

[6] (https://forobs.jrc.ec.europa.eu/TMF/explorer.php)

observations per year or 5 years with at least 2 valid observations per year). The initial reference date depends on the Landsat data availability and range from 1982 for Brazil to 2016 for Gabon.

Then, pixels are classified in seven main trajectories classes using the full single-date temporal sequence of each pixel. Each trajectory is defined by a particular chain of event. As an example, to classify a pixel as "Degraded Forest," a pixel initially classified as moist forest needs to experience a FD period smaller than 2.5 year followed by at least 3 years of regrowth. If the FD period is lower than 1 year, transition class is set at "Short-duration Degradation". If the FD period is higher than 2.5 year and not followed by a 3 year of regrowth, transition class is set at "Deforestation". Finally, if the FD period is higher than 2.5 year and is followed by at least 3 year of regrowth, transition class is set at "Forest Regrowth". Similar set of rules are defined for the four other trajectory classes. This second classification produces maps that allow to monitor the forest trajectory for a given period. More precise subclasses are added using ancillary data like the "Deforestation" class that are subclassified in three regarding the land cover in which TMF was transformed (conversion into water, plantation, or other land cover). FD pixels are also subclassed given their respective start dates, intensity, and duration. Those last steps conclude the creation of a 52-classe **transition maps**.

Finally, an annual forest change product can be computed combining the transition map with five additional layers. "The number of disruption observations per year, the first and last year of a disturbance period, the recurrence of disruption observations, the start year of the archive (first year after the initial period), and the number of valid observations per year" (Vancutsem et al., 2020). Those information's are used to define additional classification rules (no described in this document) that will create 30 **annual transition maps**.

TMF products and source codes are available at the European commission website[7]

Validation and Results

Vancutsem *et al* (2022a) use Landsat image interpretation to collect validation samples on GEE platform. The single-date algorithm for African moist forest classification has an excellent overall accuracy of 94%.

The resulting products provides an unprecedented mapping of annual FD. For the first time, a pan-tropical operational product covers the intensity, duration, sequential dynamics and start date of a degradations, tracking disturbances over time.

Evaluation

As the current version of TMF was released in 2021, no independent global evaluation has been conducted yet. However, TMF products have already been used for local application like monitoring the traceability of the Ivorian Cocoa Supply Chain (Renier et al., 2022) or Indonesian mangrove monitoring (Gomez et al., 2022).

Local study cases highlight the strong limitation of TMF particularly in the Gulf of Guinea region where it has a user's accuracy of 34.9% and a producer's accuracy of 82%. In the same study, Hansen *et al*. (2022) suggest that radar-based method outperform TMF in local use cases.

Gomez, M. ***Examining the protective services of mangroves at a regional scale in Indonesia.*** Division of risk management and societal safety, Lund University, Sweden, Thesis (2022); https://lup.lub.lu.se/luur/download?func=downloadFileandrecordOId=9099286andfileOId=9099287

[7] (https://forobs.jrc.ec.europa.eu/TMF/data.php)

Hansen, J. N.; Mitchard, E. T.A.; King S. ***Detecting Deforestation from Sentinel-1 Data in the Absence of Reliable Reference Data.*** arXivLabs (2022); https://doi.org/10.48550/arXiv.2205.12131

Renier, C. et al. ***Transparency, traceability, and deforestation in the Ivorian cocoa supply chain.*** agriRxiv. CABI International agriRxiv (2022); https://doi.org/10.31220/agriRxiv.2022.00156

Vancutsem, C.; Achard, F.; Pekel, J.-F.; Vieilledent, G.; Carboni, S.; Simonetti, D.; Marelli, A.; Gallego, J. ***Long-term monitoring of tropical moist forest extent (from 1990 to 2019).*** EUR 30448 EN, Publications Office of the European Union, Luxembourg, 2020, ISBN 978-92-76-25320-4, https://doi.org/10.2760/70243JRC122307

Vancutsem, C.; Achard, F.; Pekel, J.-F.; Vieilledent, G.; Carboni, S.; Simonetti, D.; Marelli, A.; Gallego, J. ***Supplementary materials for: Long-term monitoring of tropical moist forest extent (from 1990 to 2019).*** EUR 30448 EN, Publications Office of the European Union, Luxembourg, 2020, ISBN 978-92-76-25320-4, https://doi.org/10.2760/70243JRC122307

2.3 RADD (Radar for Detecting Deforestation)

Presentation

RADD is a conservative operational 10 m spatial resolution C-SAR based FD alert system. It aims to monitor disturbance events at a pan-tropical scale in near real time (NRT) with minimum false positive detections using probabilistic algorithms. This product is currently freely accessible as an "Integrated deforestation alerts" on the GFW online platform[8]. The system is running on GEE platform, but source codes are only available on demand.

Key concept definition

Forest is defined as an area containing more than 50% of tree canopy cover at the beginning of the detection period within an area of 0,01 ha (10 x 10 m Sentinel-1 pixel) while **forest disturbance (FD)** is defined as the partial to total tree canopy removal for the same area. This product does not distinguish natural FD (seasonal fires, landslides, …) from anthropic FD. Since the goal is to provide a FD alert, the study implicitly considers **deforestation** and **degradation** as undistinguished events. Forest and FD also have an informal probabilistic definition detailed in the methodology section.

Reich *et al* (2016) derive the initial **forest extent** for the detection period using Hansen *et al* (2013) Tree Cover product for the year 2000 and removing all historical forest cover losses detected since 2000 by the Global Forest Change operational product Hansen *et al* (2013). All data are available on the GEE GLAD online application[9]. The **tropical moist forest extent** is obtained by removing dry forest using the BuchHorn *et al* (2020) Copernicus Global Land Cover dataset[10]. Finally, small forest extent errors are removed in regards with the Global TanDEM-X Forest/Non-Forest map[11].

A **confirmed alert** for a given pixel is defined as two consecutive FD detections within a 90-day period after the first FD detection. The actual detection procedure is detailed in the methodology section.

The FD alert product is updated on **daily frequency** given the Sentinel-1 image availability at the moment. Depending on the Sentinel-1 revisiting time, a FD can be detected within a maximum of 6 to 12 days. Alerts are confirmed within 12 to 90 days but more than 66% of the alert are confirmed within 24 days and more than 88% within 48 days. Due to Sentinel-1 **latency**, an alert cannot be triggered before 5 to 6 hours after data acquisition.

Input data:

RADD use only Ground Range Detected (GRD) Sentinel-1 product in interferometric wide swath acquisition mode for FD detection. Both VV and VH polarization are used in all available orbits. Those images are already located in the GEE data collection. However, RADD is highly reliant on other annual optical, and X-SAR based product to define the initial tropical forest extent from which all detections are referring to.

In addition to the GEE pre-possessing described in detail in the GEE "Sentinel-1 algorithm" section[12], GRD images have undergone commonly applied pre-possessing including a radiometric slope correction, Quegan speckle filtering, geocoding, and gamma- naught topographical normalization.

[8] https://global forestwatch.org
[9] https://glad.earthengine.app/view/global-forest-change
[10] https://land.copernicus.eu/global/products/lc
[11] https://download.geoservice.dlr.de/FNF50/
[12] https://developers.google.com/earth-engine/guides/sentinel1

In some areas, seasons can have significant effects on pixels backscattering behavior. As such, seasonal effects are removed from each newly acquired data (detection dataset) using a harmonic model fitted with a training dataset consisting of previously computed time series (Reich *et al* 2018b).

Methodology

Reich *et al* (2016) approach can be defined as pixel-based and conditionally probabilistic. First it is assumed that backscattering behaviors differs significantly both locally (pixel scale) and temporally. For those reasons, each forest pixel is characterized by its own backscattering values distribution through time. Then FD is defined as a conditional probability that a new pixel backscattering value is a non-forest using the initial forest and non-forest historical distribution for that pixel.

In order to define the backscattering value distribution of forest pixels, the median ($\tilde{x}$) and standard deviation (σ) of each pixel belonging to the tropical forest extent are computed on de-seasonalized training time series. As a result of a previous study (Reich *et al* 2018b), the forest values are following a Gaussian distribution N ($\tilde{x}, 2\sigma$). The same study shows that non-forest median can be defined as $\tilde{x} - 4\sigma$ leading to a non-forest Gaussian distribution N ($\tilde{x} - 4\sigma, 2\sigma$) (Reich *et al* 2018a). As such, each forest pixel is defined by its own forest and non-forest overlapping Gaussian backscattering values distribution.

Following the Bayes's theorem, newly processed observations are converted into conditional probability using prior forest and non-forest distribution. The previous non-forest distribution is updated with the new observation using Bayesian updating (Reich *et al* 2015). An alert is triggered when the non-forest probability is higher than 0.85 and is confirmed if higher than 0.975 (97.5% confidence) within 90 days after the first triggering. All the function used in the pixel-based Bayesian probabilistic approach can be found in the R package available on the jreiche/bayts GitHub[13].

The resulting FD alerts have a 10 m resolution. All the confirmed disturbed pixels are clustered in the eight directions. To ensure minimal false positive detections, clusters smaller than 0.1 ha (minimal mapping unit of 10 continuous pixels) are removed. The confirmation confidence is set at 97,5% for the same reason.

Validation and Results

Reich *et al* validation process involves 1100 samples classified using image interpretation of exploitable monthly PlanetScope and Sentinel-2 images. When optical images are not available, Sentinel-1 is used instead. FD events that occurred just before the beginning of the detection period (not include in the tropical forest extent because of the lack of optical images) and ambiguous boundary pixels are not considered in the accuracy assessment. The user's and producer's accuracy are respectively 97% and 95% for confirmed alert detection for FD $\geq$ 0.2 ha (not forest disturbed area). If smaller FD are included, the producer's accuracy decreases to 83%. The temporal accuracy of the system as not yet been assessed.

Evaluation

As the current version of RADD was released in 2021, no published study has already independently evaluated the global system's performances for this specific version.

However, the 2020 version (following the same methodology) is evaluated by Carstairs *et al* (2022) using a local UAV LiDAR field mission in Gabon as validation dataset. A comparison between their annual forest cover loss product (based on Sentinel-1 images) and RADD product for the year 2020 is made both with a minimal mapping unit of 0.2 ha. The results showed that RADD cumulative alert underestimate the total deforested area by factor of at least 10. This important underestimation might be

[13] https://github.com/jreiche/bayts

due to the highly conservative Reich *et al* (2016) methodology aiming to get a minimal amount of false positive detections.

Buchhorn, M.; Lesiv, M.; Tsendbazar, N. E.; Herold, M.; Bertels, L.; Smets, B. ***Copernicus global land cover layers-collection 2.*** Remote Sens. 2020, 12(6), 1044; https://doi.org/10.3390/rs12061044

Carstairs, H.; Mitchard, E.T.A.; McNicol, I.; Aquino, C.; Chezeaux, E.; Ebanega, M.O.; Dikongo, A.M.; Disney, M. ***Sentinel-1 Shadows Used to Quantify Canopy Loss from Selective Logging in Gabon.*** Remote Sens. 2022, 14, 4233 ; https://doi.org/10.3390/rs14174233

Hansen, M. C.; Potapov, P. V.; Moore, R.; Hancher, M. et al. ***High-resolution global maps of 21st-century forest cover change.*** Science 342 850–. 2013; https://doi.org/10.1126/science.1244693

Hansen, M. C.; Krylov, A.; Tyukavina, A.; Potapov, P. V.; Turubanova, S.; Zutta, B.; Ifo, S,; Margono, B.; Stolle, F.; Moore, R. ***Humid tropical forest disturbance alerts using Landsat data.*** Environ. Res. Lett. 11 34008. 2016; https://doi.org/10.1088/1748-9326/11/3/034008

Reiche, J.; Mullissa, A.; Slagter B.; Gou, Y.; Tsendbazar, N.; Odongo-Braun, C.; Vollrath, A. et al. ***Forest disturbance alerts for the Congo Basin using Sentinel-1.*** Environ. Res. Lett. 16 024005. 2021; https://doi.org/10.1088/1748-9326/abd0a8.

Reich, J.; Hamunyela, E.; Verbesselt, J.; Hoekman, D.; Herold, M. ***Improving near-real time deforestation monitoring in tropical dry forests by combining dense Sentinel-1 time series with Landsat and ALOS-2 PALSAR-2***. Remote Sensing of Environment, Volume 204, 2018a, Pages 147-161, ISSN 0034-4257; https://doi.org/10.1016/j.rse.2017.10.034.

Reiche, J.; Verhoeven, R.; Verbesselt, J.; Hamunyela, E.; Wielaard, N.; Herold, M. ***Characterizing Tropical Forest Cover Loss Using Dense Sentinel-1 Data and Active Fire Alerts***. Remote Sens. 2018b, 10, 777; https://doi.org/10.3390/rs10050777

Reiche, J.; de Bruin, S.; Hoekman, D.; Verbesselt, J.; Herold, M. ***A Bayesian Approach to Combine Landsat and ALOS PALSAR Time Series for Near Real-Time Deforestation Detection Remote Sens***. 2015, 7, 4973-4996; https://doi.org/10.3390/rs70504973

2.4 Global Analysis and Discovery Forest Loss Alerts

Presentation

Global Analysis and Discovery laboratory Forest Loss Alerts product (GLADa) is a conservative operational 30 m spatial resolution optical based forest disturbance alert system. It claims to monitor disturbance events at a pan-tropical scale in near real time. It was developed in 2016 and annually updated by the Department of Geographical Sciences in the University of Maryland (UMD) in the GLAD laboratory. This product is currently freely accessible as an "Integrated deforestation alerts" on the Global Forest Watch (GFW) online platform[14]. The system is running on GEE.

Key concept definition

Forest is defined as an area containing more than 30% of tree canopy cover (minimal height of 5 m) at the beginning of the detection period within an area of 0,09 ha (30 x 30 m Landsat pixel) while **FD** is defined as the removal of at least 50% of the initial tree canopy for the same area. This product does not distinguish natural FD (seasonal fires, landslides,…) from anthropic FD. Since the goal is to provide an FD alert, the system implicitly considers **deforestation** and **degradation** as undistinguished events.

Hansen *et al* (2016) derive the initial **forest extent** for the detection period using pre-existing humid tropical forest local map for the year 2000 and removing all historical forest cover losses detected since 2000 by the Global Forest Change operational product Hansen *et al* (2013).

A **confirmed alert** for a given pixel is defined as at least two FD detections within four consecutive observations, the first FD detection being the first of the four observations. The actual detection procedure is detailed in the methodology section.

The FD alert product is updated on **daily frequency** given the Landsat image availability at the moment. In addition to the 16 days Landsat revisiting time, the **latency** between the alert and the actual FD event can be severally expand due to dense cloud coverage leading to a lack of exploitable optical images. For those reasons, an alert can be triggered from 16 days up to half a year after the actual FD; some areas being covered only during dry season.

Input data

GLADa use images coming from both the ETM+ instrument from Landsat 7 (bands 3, 4, 5 and 7) and the OLI from Landsat 8 (bands 4, 5, 6 and 7) for the FD detection process. Normalized difference vegetation index (NDVI), NDWI, Normalized Burned Ration (NBR), ETM+ band 6 and the TIR band 10 are used for time series metrics.

Radiometric normalization is implemented on every observation using top-of-atmosphere reflectance and their corresponding Moderate Resolution Imaging Spectroradiometer (MODIS) imagery for radiometric adjustment.

The newest version of GLADa called GLAD-S2 using Sentinel-2 images is currently available in GFW platform. For now, no paper describes the specificities of this recent version, but it is assumed that the methodology, aside from data pre-possessing and spatial resolution, is more or less the same.

Methodology

In order to characterized undisturbed forest and FD, 4-year time series are computed, and several metrics are extracted including mean band values, regression slope and composites values. Those metrics are used as features to train a generic bagged decision trees classification algorithm in order to segregate FD from stable forest on a pan-tropical scale. After analysis, new observations are added to the time

[14] (https://global forestwatch.org)

series and metrics are updated. The algorithm is trained using 953.000 pixels acquired by Landsat image interpretation. The algorithm is iteratively optimized until a stable model is obtained.

Three set of this bagged trees are computed, each model input the latest Landsat image, use the previously updated time series metrics to train themselves, output a value corresponding to the likelihood FD and finally update the metrics with the new observation. The median likelihood obtained for the three models is calculated. If the median is > 50%, an alert is triggered, if for the same location an alert is triggered again by the three following observations, a confirmed alert is declared.

The latest version of GLADa "Landsat ARD tools" used for this study are freely available as QGis extension and R packages at the GLADa web site Software section[15].

In contrast with RADD methodology, GLADa alert-pixels are not clustered leading to a substantial number of unrelated pixels which might be hard to analyze at local level. To overcome this issue, a clustering product was developed by Goodman (2016) using GEE and GFW GLADa data.

Due to its conservative approach, GLADa alert is dedicated to providing NRT alerts with minimal false positive at the known cost of severe FD area underestimation, therefore the model is not meant to ensure proper annual forest cover loss area calculation. All GLADa alerts are freely accessible at the GLAD Forest Loss Alert online application[16].

Validation and Results

Hansen *et al* (2016) first validation process is conducted on the Peru Tropical Forest during the year 2014. Around 1300 validation samples are collected and labelled using Landsat image interpretation. With a user's accuracy of 99% and a producer's accuracy of 69%, the method is truly conservative with an expected high amount of omissions errors.

A comparison is also made between the Hansen *et al* (2013) annual tree cover loss map available in the GFW platform for Peru, Republic of Congo and Indonesia and the cumulative FD area detected. As expected, FD alerts are predominant during the dry season following the higher optical data availability during this period. Results confirm the conservativeness of this FD detection method, with the notable exception of the Congolese forest where only 21% of the deforested area detected by GFW are also detected by GLADa. This low performance might be explained by the difficulties to identify small FD patches which are predominant in the Congo Bassin and the lack of recurrent exploitable optical data in this area.

Evaluation

Bouvet et al (2018) highlight that for small FD area detection, S1-based methods are always superior in comparison with GLADa both in detection rate and speed. Especially for FD area smaller than 1 ha where only 80% of the FD are detected by GLADa. However, GLADa achieved a 100% detection rate for FD bigger than 3 ha. Further study demonstrates the strong limitation of GLADa during wet season leading to important FD area underestimation (Araza *et al*,2021) especially in FD events happening outside of the deforestation hotspots.

It is demonstrated that subscription to GLADa alert system by local actors is correlated with the decrease in deforestation in their operational area. As so, global NRT FD systems are proven beneficial for tropical forest conservation. Especially in Africa where the use of GLADa "led to an 18% decrease in the probability of forest loss" (Moffette et al., 2021).

[15] https://glad.umd.edu/ard/software-download
[16] http://glad-forest-alert.appspot.com

Araza, A.B.; Castillo, G.B.; Buduan, E.D.; Hein, L.; Herold, M.; Reiche, J.; Gou, Y.; Villaluz, M.G.Q.; Razal, R.A. ***Intra-Annual Identification of Local Deforestation Hotspots in the Philippines Using Earth Observation Products***. Forests 2021, 12, 1008; https://doi.org/10.3390/f12081008

Bouvet, A.; Mermoz, S.; Ballère, M.; Koleck, T.; Le Toan, T. ***Use of the SAR Shadowing Effect for Deforestation Detection with Sentinel-1 Time Series.*** Remote Sens. 2018, 10, 1250; https://doi.org/10.3390/rs10081250

Hansen, M. C.; Potapov, P. V.; Moore, R.; Hancher, M. et al. ***High-resolution global maps of 21st-century forest cover change.*** Science 342 850–. 2013; https://doi.org/10.1126/science.1244693

Hansen, M. C.; Krylov, A.; Tyukavina, A.; Potapov, P. V.; Turubanova, S.; Zutta, B.; Ifo, S,; Margono, B.; Stolle, F.; Moore, R. ***Humid tropical forest disturbance alerts using Landsat data.*** Environ. Res. Lett. 11 34008. 2016; https://doi.org/10.1088/1748-9326/11/3/034008

Goodman, C. ***Triaging deforestation alerts: Clustering alerts for review.*** 2016 IEEE Global Humanitarian Technology Conference (GHTC); https://doi.org/10.1109/GHTC.2016.7857264

Moffette, F.; Alix-Garcia, J.; Shea, K.; Pickens, A. ***The impact of near-real-time deforestation alerts across the tropics.*** Nature Climate Change. VOL 11. February 2021. 172–178; https://doi.org/10.1038/s41558-020-00956-w

2.5 DETER-R (DETERring Deforestation in the Amazon using Radar images)

Presentation

DETER-R is an operational 10 m spatial resolution C-SAR based FD alert system. It aims to monitor FD events for the Amazon humid tropical forest in NRT using an Adaptative Linear Thresholding (ALT) method. DETER-R is conducted by the Brazilian National Institute for Space Research (INPE) alongside two other monitoring systems, the Brazilian Amazon Rainforest Monitoring Program by Satellite (PRODES) and the Brazilian land use and land cover mapping system (TerraClass). DETER-R is currently running on a GEE online platform.

Key concepts definition

Forest and forest disturbance are not rigorously defined in DETER-R related publications. However, all forest pixels are characterized by a 3-year (training period) median backscattering value and an associated negative threshold computed considering the pixel distance from the closest deforested area. A **forest disturbance** happens when the new pixel backscattering value is smaller than the difference between its 3-year historical median and its threshold value.

Doblas *et al* (2022a) derive the initial **forest extent** for the detection period by combining multiple pre-existing forest maps. First the main forest extent was extracted by adding the Landsat-based deforestation map[17] from PRODES to the visual-interpretation-based forest/non forest map[18] from INPE. Small farmland and savanna patches are removed using the Global TerraSAR-X forest/non forest map[19]. Finally, seasonally flooded forests and coastline forests extents are removed from the final **tropical forest extent** to avoid false positive detections. Those forest extents are coming respectively from the INPE's varzea extent[20] and the data from Geomorfolia map[21] published by the Brazilian Institute from Geography and Statistics (IBGE).

A **confirmed alert** for a given pixel is defined as the detection of at least two FD events in a two-month period (detection period). The actual detection procedure is detailed in the methodology section.

The FD alert product is updated on **daily frequency** given the Sentinel-1 image availability at the moment. Given the 6 to 12 days Sentinel-1 revisiting time and the **latency** between the image acquisition and its availability on GEE (delay up to more than 60), the delay between FD and a confirmed alert is ranging from 6 to 75 days with 50% of the alert being confirmed within 23 days delay. In the normal operation condition, GEE latency should not be as high and so Doblas *et al (2020)* claim an expected nominal delay of 18 days after the FD.

Input data

DETER-R only use GRD Sentinel-1 product in interferometric wide swath acquisition mode for FD detection. VH polarization is used in all available orbits. Those images are already located in the GEE data collection. However, DETER-R is highly reliant on other annual optical and X-SAR based product to define the initial tropical forest extent from which all the detection are referring.

DETER-R input data followed the same pre-possessing applied by the RADD system. In addition to the GEE pre-possessing described in detail in the GEE "Sentinel-1 algorithm" section[22], GRD images have

[17] http://www.obt.inpe.br/OBT/assuntos/programas/amazonia/prodes
[18] http://terrabrasilis.dpi.inpe.br/en/download-2/
[19] https://download.geoservice.dlr.de/FNF50/
[20] http://terrabrasilis.dpi.inpe.br/en/download-2/
[21] https://www.ibge.gov.br/geociencias/informacoes-ambientais/geomorfologia/10870-geomorfologia.html
[22] https://developers.google.com/earth-engine/guides/sentinel1

undergone several commonly applied pre-processing including a radiometric slope correction, Quegan speckle filtering, geocoding, and gamma-naught topographical normalization. The data was also de-seasonalized using the harmonic stabilization technique (Reich *et al* 2018b) described in RADD section.

Methodology

The ALT methodology used by DETER-R is described in detail by Doblas *et al* (2020). Still a succinct explanation is provided. The idea of DETER-R system is to characterize the probability of new pixel being a FD as a function of its Euclidian distance from the nearest deforested areas. This function input a distance *d* and output a threshold value *t* unique to each pixel following a logistic distribution $t\ (d;\ t_0;\ t_{max};\ \mu,\ s)$ presented in (1). With t_{max} being the maximal *t* value associated to a distance of at least 10 km from the nearest deforested pixel and t_0 being the minimal *t* value associated to the pixel limiting a deforested area. The μ and *s* location and scale parameter are fitted to historical data using *fitdistplus* R library.

(1) $$t(d;\ t0;\ tmax;\ \mu, s\ ) = d_0 + (t_{max} - t_0)\left(\frac{1}{2} + \frac{1}{2}\tanh\left(\frac{log_{10}(d) - \mu}{2s}\right)\right)$$

For each pixel, the 3-year median *m* value is computed. When a backscattering value γ^0_{VH} confirmed the equation (2), an alert is triggered; when it is confirmed at least twice during the two-month detection period, an alert is confirmed.

(2) $$m\ -\ t(d;\ t0;\ tmax;\ \mu, s\ ) < \gamma^0_{VH}$$

All confirmed detections are clustered in FD polygons. Those are characterized by their number of pixels, the mode of the first detection date on the detection collection and finally the median value of the difference between the backscattering value and the threshold of the detection collection. This last characteristic allowed the model to classify Low and High intensity FD.

Finally, in order to obtain minimal false positive and to fulfil stakeholder demand, the minimum mapping unit was set to 1 ha.

All the codes used to develop DETER-R are open-source and available in the J. Doblas GitHub[23].

Validation and Results

Doblas *et al* (2022a) operational validation process is conducted in the Amazon Forest using the annual PRODES deforestation map and field data. Despite high confusion between high and low intensity classes, DETER-R claims a high user's accuracy of 96%. However, DETER-R has a high FD omission rate with a producer's accuracy of 50%. This high omission rate was expected given the objective of minimizing false positive detections. Further study highlights the fact that the current methodology can be optimized leading to better producer's accuracy might be obtained at the cost of a lower user's accuracy (Doblas *et al*., 2022b) and so DETER-R performances might increase in further update.

Evaluation

As the current version of DETER-R was released in 2022, no published study has already independently evaluated the system performances for this specific version. However, Convolutional Neural Network (CNN) has proven to produce better results than ALT for FD detection in the Amazon tropical forest (Ortega et al., 2022) outperforming the ALT methodology.

Pending future publications, we can assume that DETER-R methodology on its own might not be fully adequate for the Congo Bassin FD specificity (high amount of small FD patches). In fact, DETER-R is

[23] https://github.com/jdoblas/DETER_R_AMZ

not designed to monitor small FD regarding its large minimal mapping unit necessary to achieve good detection rate.

In this review, it was chosen not to describe previous INPE alert systems DETER and DETER-B (Diniz *et al*., 2015) launched respectively in 2004 and 2015 because of their outdated 250 m resolution in comparison with more high-resolution state of the art NRT detection systems like RADD or GLAD.

Doblas, J.; Reis, M.S.; Belluzzo, A.P.; Quadros, C.B.; Moraes, D.R.V.; Almeida, C.A.; Maurano, L.E.P.; Carvalho, A.F.A.; Sant'Anna, S.J.S.; Shimabukuro, Y.E. ***DETER-R: An Operational Near-Real Time Forest Disturbance Warning System Based on Sentinel-1 Time Series Analysis***. Remote Sens. 2022a, 14, 3658; https://doi.org/10.3390/rs14153658

Doblas, J.; Shimabukuro, Y.; Sant'Anna, S.; Carneiro, A.; Aragão, L.; Almeida, C. ***Optimizing Near Real-Time Detection of Deforestation on Tropical Rainforests Using Sentinel-1 Data***. Remote Sens. 2020, 12, 3922; https://doi.org/10.3390/rs12233922

Doblas, J.; Lima, L.; Mermoz, S.; Bouvet, A.; Reiche, J.; Watanabe, M.; Sant'Anna, S.; Shimabukuro, Y. ***Inter-comparison of optical and SAR-based forest disturbance warning systems in the Amazon shows the potential of combined SAR-optical monitoring***. Int. J. Remote Sens. 2022b; submitted

Diniz, C.G.; Souza, A.A.D.A.; Santos, D.C.; Dias, M.C.; Luz, N.C.D.; Moraes, D.R.V.D.; Maia, J.S.A.; Gomes, A.R.; Narvaes, I.D.S.; Valeriano, D.M.; et al. ***DETER-B: The New Amazon Near Real-Time Deforestation Detection System***. IEEE J. Sel. Top. Appl. Earth Obs. Remote Sens. 2015, 8, 3619–3628; https://doi.org/10.1109/JSTARS.2015.2437075

Ortega Adarme, M.; Doblas Prieto, J.; Queiroz Feitosa, R.; De Almeida, C.A. ***Improving Deforestation Detection on Tropical Rainforests Using Sentinel-1 Data and Convolutional Neural Networks***. Remote Sens. 2022, 14, 3290; https://doi.org/10.3390/rs14143290

2.6 TropiSCO (Tropical Space for Climate Observatory)

Presentation

Tropisco is an operational 10 m spatial resolution C-SAR based FD alert system. It is currently monitoring disturbance events in NRT for French Guyana, South-East Asia and Gabon using SAR-shadowing effect among its methodology. In near future, Tropisco aims to monitor FD at a pan-tropical scale. TropiSCO is developed by the Space for Climate Observatory (SCO) in close collaboration with the Centre d'Etudes Spatiales de la Biosphère (CESBIO) and the Centre National d'Etudes Spatiales (CNES). Since 2022 this product is freely available and downloadable on the TropiSCO interactive online platform[24]. It is noteworthy that unlike all operational NRT FD monitoring systems, TropiSCO is not running on a GEE online application.

Key concepts definition

Forest and forest disturbance are not rigorously defined in TropiSCO technical descriptions and related publications. However, Bouvet et al (2018) compared extensively their results with GLAD systems. As such we can assume that they have a similar definition. **Forest** is defined as an area containing more than 50% of tree canopy cover (minimal height of 5 m) at the beginning of the detection period within an area of 0,01 ha (10 x 10 m Sentinel-1 pixel) while **forest disturbance** is defined as tree cover removal event leading to a tree cover of <10%. This product does not distinguish natural FD (seasonal fires, landslides, …) from anthropic FD. Since the goal is to provide FD alert, the system implicitly considers **deforestation** and **degradation** as undistinguished events.

Bouvet et al (2018) methodology does not require (but recommend) to restraint the **forest extent** in order to produce proper FD alerts and does not provide a generic initial extent on which the detection is conducted. However, in particular areas where steep slopes are prominent, it is strongly recommended to restrain the detection extent to flat/lightly hilly terrains (not more than 20% steep slopes for average forest height of at least 25m) as shadow detection is slope dependent. Slope effect on the detection extent is detailed in the methodology section.

An **alert** is triggered and confirmed if a sudden drop in backscattering value happens between two consecutive observations. A more complex definition as well as a way to define the drop intensity needed to trigger an alert is described in the methodology section.

The FD alert product is updated on **daily frequency** following the Sentinel-1 image availability at the moment. Given the 6 to 12 days Sentinel-1 revisiting time and the time needed to detect shadows after a FD event, the **latency** between FD and FD alert is at least 12-24 days but not more than 18-36 days for most cases (including Congo Bassin region).

Input data:

TropiSCO uses only GRD Sentinel-1 products in interferometric wide swath acquisition mode for FD detection. VH polarization is used in all available orbits. VH is prefer due to better VH performances over VV on steep slopes. Those images are downloaded using the Sentinel Product Exploitation Platform[25] (PEPs) online platform proposed by the CNES.

GRD images have undergone commonly applied pre-possessing including a radiometric slope correction, Quegan speckle filtering, geocoding using Orfeo Toolbox[26] (OTB) and gamma-naught topographical normalization using the Shuttle Radar Topography Mission (SRTM).

[24] https://www.tropisco.org/
[25] https://www.peps.cnes.fr/
[26] https://www.orfeo.toolbox.org/

Methodology

Tropisco methodology is divided in two steps. First a shadow is detected, then the correspondent deforested area is reconstructed using the shadow patches extents.

SAR-shadows detection relies on a purely geometrical feature coming from Sentinel-1 incidence angle (θ). In fact, after FD events, areas that were previously observed by Sentinel-1signal are now hidden by the surrounded canopy. If the surrounding trees height (H) is sufficient, a persistent significative decrease in backscatter is expected. Shadow's width (W) follows the equation (1). In order to be detectable, a shadow must be at least 1,5 Sentinel-1 pixel or 15 m wide. As such, in the worst case (when θ = 29°) trees must be at least 27 m height; in the best case (when θ = 46°) trees must be at least 14 m height.

(1) $W = H\,tan(\theta)$

(2) $K = \cos(\theta)(\cos(\alpha)/\cos(\theta - \alpha))$

(3a) $\alpha < 0$ if slope oriented away from the sensor

(3b) $\alpha > 0$ if slope oriented towards the sensor

Those restrictions are furthermore tightening by the effect of slope (α) on shadows width. The shadow width is multiplied by a K factor (2) given the slope orientation. If the slope is oriented towards the sensor (3b), the shadow width will decrease, if not (3a) it will increase. For a strong slope of 17° (20% steep) in the worst case, the shadow width will decrease from 15%. In order to be detectable in the worst and best case, the minimal tree height must be respectively 31 m and 17 m. For that reason, it is strongly recommended to restrict the detection extent to dense forest with tall trees located not/lightly hilly terrain.

The Radar Change Ratio (RCR) is used to detect sudden drops in backscattering associated with the occurrence of shadows. For a given pixel, RCR is computed as the ratio between the mean backscattering value of a one-month detection period and the historical mean backscattering value. An alert is triggered when RCR is $\leq$ to a certain threshold value (depending on the study area). If an alert is not triggered, data used during the detection period are used to compute new historical mean, and the three next observation serves as a new detection period. Only shadow segment $\geq$ 0.04 ha are kept removing small outliers.

Previously detected shadows are used to reconstruct deforested areas. The shadow's neighboring pixels that experience a decrease in backscattering of at least -3 dB during the detection period are clustered together with the shadowed pixels. Only shadow segment $\geq$ 0.1 ha are kept removing small outliers setting the final minimal mapping unit. The obtained patches are then slightly shrank using the MATLAB *Boundary* [27] function. Even if this procedure is applicable using only one orbits, it produces better results using both ascending and descending orbits.

Given this methodology, the system is expected to perform well at detecting small FD patches in priority. In fact, big FD events might not produce sufficient shadows to properly reconstruct the entire FD area.

All TropiSCO alerts are freely accessible on the TropiSCO online application[28].

Validation and Results

The first validation is conducted on the Peruvian tropical forest using the only two cloud free Sentinel-2 images. A set of deforested areas are collected using optical images visual interpretation. This set is than use to train a decision tree algorithm which will automatically collect hundreds of sample points. Those sample are then visually checked. With a user's accuracy of 99.4% and producer's accuracy of 80.3%, SAR-shadowing methodology outperformed all previous SAR-based FD detection. It is worth noting that Peru is covered by both ascending and descending orbits. Further study show that the results

[27] https://fr.mathworks.com/help/matlab/ref/boundary.html
[28] https://www.tropisco.org/telechargement

are more mixed when it comes to monitoring the area covered by a single orbit (as it is the cas for the Congo Bassin region).

Evaluation

As the current version of TropiSCO was released in October 2022, no published study has already independently evaluated the system's performances. However, multiple operational validation has been conducted by their developers in various tropical countries since the first prototype of SAR-shadowing based methodology (2018).

In 2021, the methodology was evaluated in Laos, Cambodia and Viet-Nam using both orbits. The results show similar user's accuracy and an even better producer's accuracy of 89%. This study also demonstrate that SAR-shadowing methodology can be used to provide weekly, monthly, and annual FD reliable statistics both in alert number and extent (Mermoz *et al*., 2021). At the moment, TropiSCO is the only operational system that achieved to combine accurate FD area measurement and low false positive and negative FD detection in NRT.

A validation was conducted on Gabon (Hirschmugl *et al*., 2020) using a forest mask to define the prior forest extent. The user's accuracy for small FD event ($\leq$ 25 ha) is 80% and the producer's accuracy is 61%. Those mixed results mitigate the methodology efficiency for the Central African region which is only covered by a single orbit and offers different FD dynamics than for South-East Asia or Peru.

Bouvet, A.; Mermoz, S.; Ballère, M.; Koleck, T.; Le Toan, T. ***Use of the SAR Shadowing Effect for Deforestation Detection with Sentinel-1 Time Series***. Remote Sens. 2018, 10, 1250; https://doi.org/10.3390/rs10081250

Hirschmugl, M.; Deutscher, J.; Sobe, C.; Bouvet, A.; Mermoz, S.; Schardt, M. ***Use of SAR and Optical Time Series for Tropical Forest Disturbance Mapping***. Remote Sens. 2020, 12, 727; https://doi.org/10.3390/rs12040727

Mermoz, S.; Bouvet, A.; Koleck, T.; Ballère, M.; Le Toan, T. ***Continuous Detection of Forest Loss in Vietnam, Laos, and Cambodia Using Sentinel-1 Data***. Remote Sens. 2021, 13, 4877; https://doi.org/10.3390/rs13234877

2.7 Current paradigms, caveats, and possible improvements

The large scale near-real-time tropical forest disturbance monitoring is currently provided by four operational systems. The three most recent systems, RADD (2021), DETER-R (2022) and TropiSCO (2022), use Sentinel-1 SAR data while the older GLADa (2016) system use Landsat/Sentinel-2 optical data.

In a tropical context, SAR-based detection always outperformed the optical-based system in temporal resolution regardless of the methodology. Given the excellent GLAD results in non-tropical region, it is assumed that the lack of exploitable optical data, more that the methodology, limits GLAD performances in those areas. Optical data unavailability is a well-known problem over the tropical moist forest and is mainly due to atmospheric disturbance. Considering that this cloud-linked-limitation will never be overcome, and that the temporal resolution is a crucial asset for an alert system, it is not surprising that most recent systems consistently prioritized SAR data. That being said, the current trend tends to call for the development of hybrid monitoring systems combining SAR and optical data. This is furthermore enhanced by the demonstrated complementarity of optical and SAR detections.

This shortage in optical data might also have a side effect on radar-based system validation which usually use optical data to collect samples, as radar images are harder to visually interpret. This might produce a bias in NRT FD system validation and create a situation where only valid optical data are used to both validate and train detection models and thus underestimates brief FD events without even noticing it (error propagation due to high correlation between calibration and validation input data). In order to mitigate these potential threats, it might be useful to develop reliable visual interpretation sampling methods based on radar images/composites in parallel of optical based sampling.

Global high-resolution radar-based systems could not be developed before 2015 due to a lack of reliable and consistent data sources. This limitation was overcome with the launching of Sentinel missions. The fact that Congo Bassin experiences a Sentinel-1 revisiting time of 12 days in only one orbital direction most of the time severely damage both temporal and spatial accuracy of the tree radar-based systems. This limitation is reinforced for the TropiSCO system which relies on ascending and descending orbits to produce its best results. As such, it appears that tropical regions, and in particular Congo bassin tropical moist forests, are among the least covered area while experiencing widespread deforestation and covering a huge and often poorly accessible surface.

Every NRT FD monitoring system relies on a reference forest extent in order to begin the actual FD detection. While most systems use already existing global forest mask like the one from GFC, it is highly recommended to perform at least a local calibration on existing product as using a global product at local scale generate non-neglectable errors that might propagate further to the system.

Regardless of the input data, time series analysis seems to be the most relevant approach to achieve proper detection. Those are widely used by all systems for signal behaviours characterization, metrics computation, model calibration, and/or data pre-processing. Time series analysis is considered as the most effective way to avoid errors coming from the signal temporal inconsistency. Depending on the data type, those inconsistencies are mainly caused by speckle, seasonality, or atmospheric disturbances. As such, it is highly recommended to use/improve time series metrics in future detection systems.

All systems with the exception of DETER-R provide free access to their NRT and annual FD records for the Congo Bassin region, opening the way for a consolidated approach combining results from various sources. It should be noticed that TropiSCO data are only available for Gabon but aims for pan-tropical mapping in the near future.

Two main kind of forest monitoring systems are operational these days. On one hand, those producing annual change detection products deliver an annual map forest change. Their algorithms varies from multidimensional clustering to bagged decision trees. In most operational systems, data driven approach

produces the best results for image analysis if and only if two requirements are fulfilled. First training samples must be numerous; this is almost always possible in annual product given the high-resolution optical data availability. Second, the metrics used as input features must be numerous and uncorrelated (the must consisting of model driven by different data sources like combining Sentinel-1 and 2). Once well calibrated, data driven approaches tend to create stable and reproductible mapping results at the cost of temporal resolution. As such, those systems do not truly detect change as a variation in signal intensity but instead as a difference between two one-year distant classification.

The second type of operational provide NRT alert (within 3 to 70 days). These do not have the luxury to afford feeding a data driven algorithm due to the lack of trustful training samples and input data scarcity. In fact, those systems use mostly expert-based calibrated threshold-based algorithm based on trial and error. When the intensity of the signal reaches a certain threshold, the FD is detected. This low data density technic increases the risk of misclassification. To counter this limitation, all systems still used time series metrics to calibrate their model by characterizing the "normal state" of stable forest and sometimes stable non-forest. Another way to increase data density is to delay detection by several days and thus using small time series. If locally calibrated, threshold-based algorithm are expected to produce better NRT results than data driven calibration. However, the annual sum of NRT detections is expected to be significantly lower than the number of detections coming from annual products as they tend to minimize the commission errors.

Given their unavoidable limitations, NRT products are designed to produce more conservative prediction as more audacious models would produce too much uncertainty and false positive. On the opposite, annual products succeed to deliver much larger extent of change while still conserving low uncertainty apparently. As a direct consequence, producer's accuracy is expected to be higher in annual product than in NRT products while user's accuracy is expected to be high in both products.

To ensure proper NRT prediction, it is critical to capitalize on previous annual products in order to start NRT detection on an updated reliable forest extent. When annual products do not detect a long-term FD, the annual change maps can still detect it the next year, while once NRT systems miss the detection of a long-term FD, it might not detect it later on. The lack of annual systems using SAR time-series as input data might explain the large discrepancies between SAR-based NRT systems and optical-based annual products. Given the current state of the art in SAR images analysis and the increasing evidence about SAR and optical complementarity for forest monitoring, it should be a priority to combine SAR and optical time-series analysis for more reliable forest monitoring systems.

3. Product comparison for the Congo Bassin long term forest monitoring

TMF and GFC are currently the only operational systems providing long term forest disturbance data in the Congo Bassin with sufficiently low omissions error so that they can be used for exhaustive deforestation mapping. Furthermore, they deliver the most popular products extensively used by national and international stakeholders. It is however important to consider that both systems are not specifically design for this purpose and that the overall cloud coverage in the region severely impact their performances both spatially and temporally. Considering that those are the only satellite-based dataset available at the moment for global long-term analysis, this section will be dedicated to assessing their strengths and caveats qualitatively and quantitatively for tropical moist forest disturbance mapping in the Commission des Forêts d'Afrique Centrale (COMIFAC) countries.

3.1 Scope of the system's comparison analysis

3.1.1 Time period

Both systems use Landsat 7 (1999-2022) and 8 (2013 onwards) archive as input dataset. In addition to those systematic acquisitions, TMF use the full L1T archive including Landsat 4 (1982-1993) and 5 (1984-2013) thematic mappers. Those two last datasets are fully compatible with Landsat 7 and 8, but their lack of systematic acquisition drastically limited the amount of available data especially in Central Africa (USGS, 2022). Given the lack of valid optical data before the launch of Landsat 7, as shown in Figure 1, it is likely that the detection algorithms based on Landsat 4 and 5 will suffer from high omission errors. This is clearly visible in the Figure 2 that shows the start of the monitoring period for each pixel of the study area for the TMF dataset. It indicates that an important part of the Congo Bassin TMF is only monitored after the year 2000 due to data scarcity in the region (up to 2013 in part of the Gulf of Guinea). It was decided to start analysing both systems from the beginning of 2001 so that both systems would have at least 1 year of data available for fair comparison. Therefore, this analysis will take place on a 20-year period from January 2001 to December 2021.

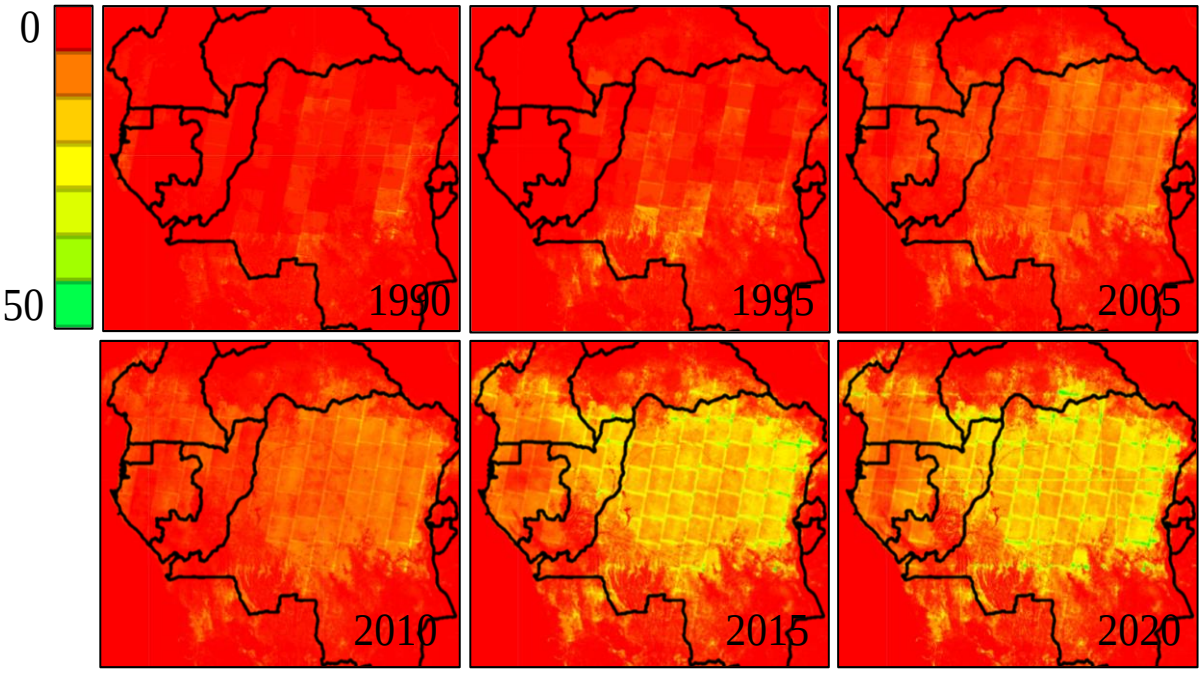

***Figure 1**: Number of annual valid observations available for forest monitoring for the TMF products from 1990 to 2020 in the Congo Bassin region. Some red areas are so not because of the lack of actual cloud free observation but because they are out of the study area (water, non-forest, …).*

Defining deforestation and degradation precisely is a complex task, especially in the Congo Basin context. In Central African tropical moist forest, important atmospheric disturbances, shifting cultivation, smallholder's clearings local or low intensity logging and fast regrowing dynamics within severely constrain the ability to detect forest change from satellite observations. In this context of gradient of forest change, the semantic boundary between degradation and deforestation is quite thin and associated with high uncertainty. It was chosen to not consider regrowth in this study. Therefore, this products comparison concerns only gross forest disturbance detections from 2001 to 2021 occurring within a common 2000 undisturbed Tropical Moist Forest extent considering that a pixel cannot regrow after any forest disturbance event (i.e. direct deforestation, degradation and deforestation after degradation are considered).

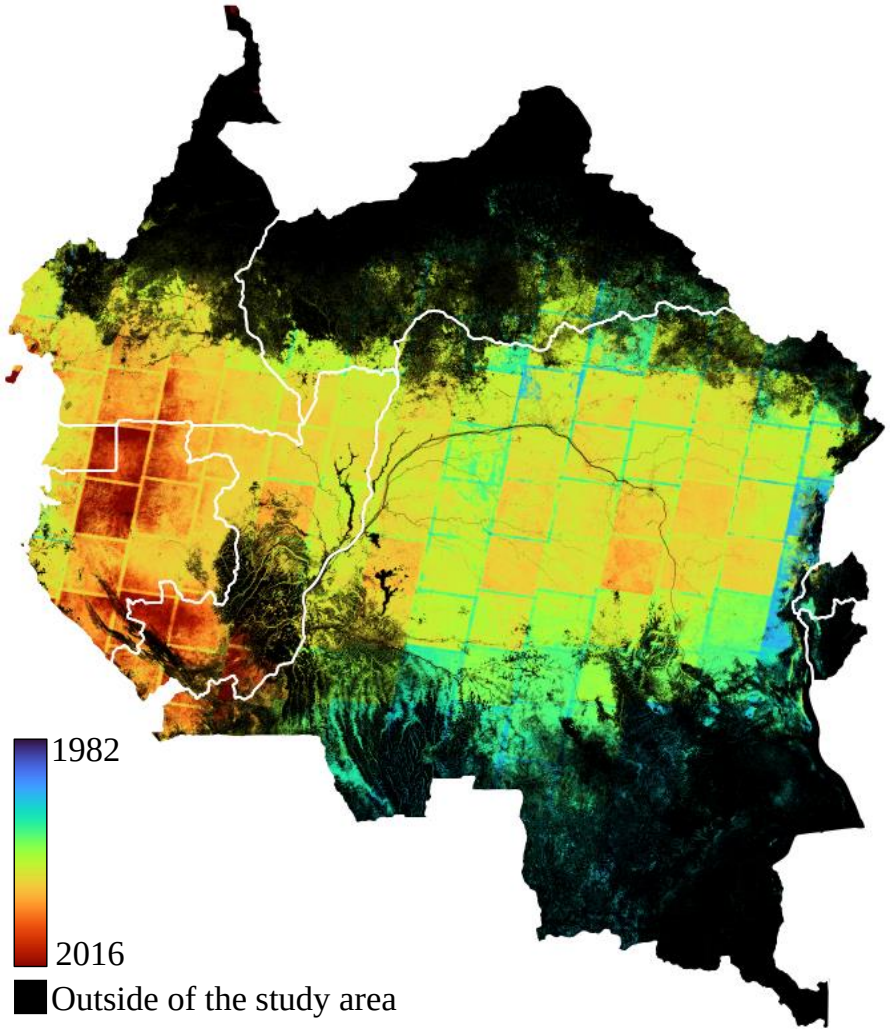

Figure 2: *Map the Congo Bassin region showing for each pixels the start date of the monitoring period for the TMF product.*

3.1.2 Forest extent definition

The detection domain defines the spatial and temporal window in which forest change is monitored. For this comparison, the time window was previously extended from 2001 to 2021 included mostly because of the Landsat data scarcity before 2001 in Central Africa.

The spatial domain of detection is the actual forest mask in which disturbance are allowed to be monitored. As this study target only undisturbed tropical moist forest, the Undisturbed tropical moist forest in the year 2000 seems to be an obvious choice for an initial forest extent. TMF defines an undisturbed forest as any closed canopy that encountered no perturbation event during the entire Landsat

archive duration. However, as shown in Figure 3, this forest extent also includes most of the fallows and secondary forest existing in the rural complex which are usually not included into the primary forest definition.

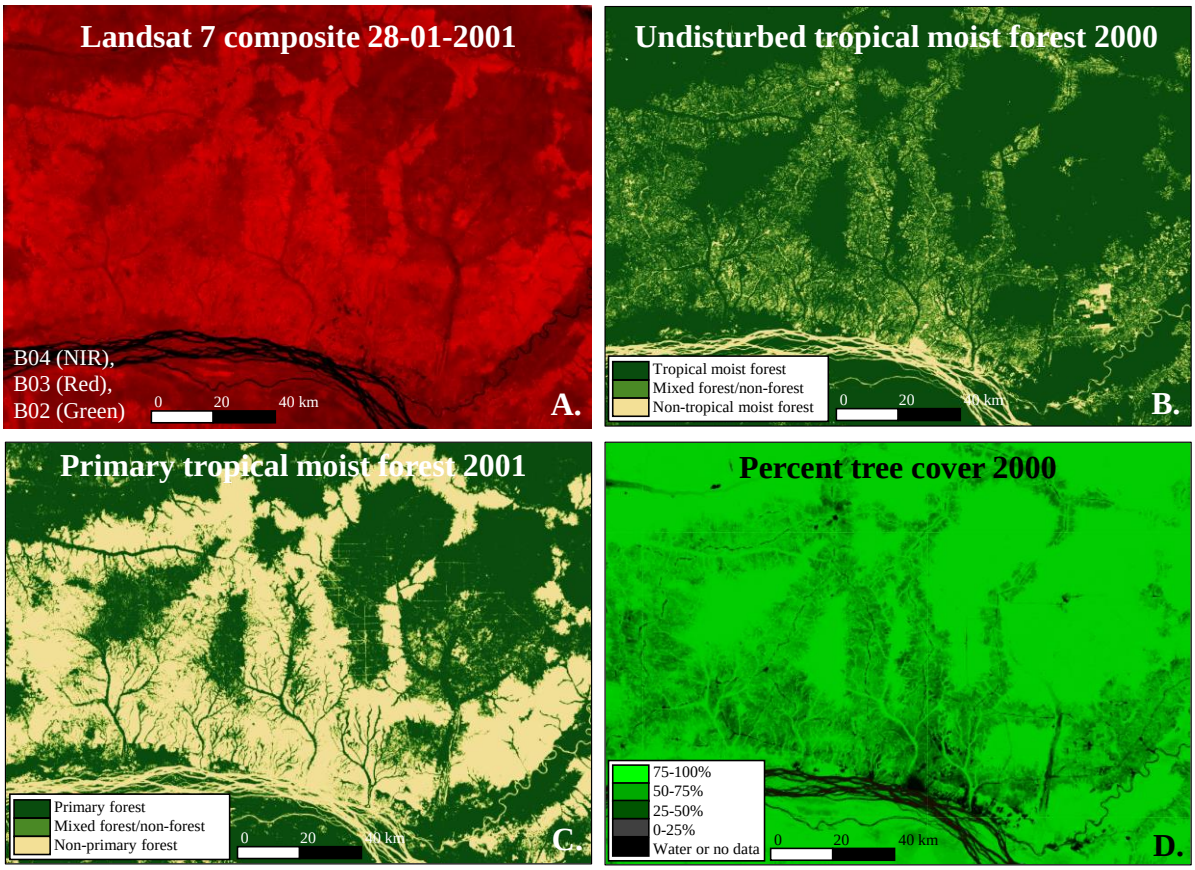

Figure 3: A. *Landsat 7 NIR, Red, Green composite from early 2001 highlighting the strong difference between highly degraded forest landscape deeply connected with the rural complex (light green) and the dense tropical moist forest (dark green).* ***B.*** *Undisturbed tropical moist forest extent for the end of 2000 using the Class 1 of the Annual Change Collection from the TMF dataset.* ***C.*** *Primary Forest extent for the year 2001 produced by the GLAD laboratory.* ***D.*** *Percent tree cover in 2000 used as forest extent for the GFC dataset.*

Considering that the rural complex and the primary forest are two separate domains for change detection, a more conservative primary forest mask was produced for our analysis. In the Figure 3C, this mask is the intersection of the undisturbed tropical moist forest mask from TMF, and the primary forest mask produced by the GLAD for the year 2001 (Turubanova et al., 2018). This mask GLAD mask excludes the rural complex and highly degraded forest extent. A study from Molinario et al., (2017) from 2000 to 2016 shows that fallows and secondary forests occupy more than half of the rural complex in the DRC and are subject to chronic low-intensity disturbances. As such, it is expected that the TMF product will produce many more detections than GFC in this area, given that clearing is less frequent (~5% of the rural complex in the DRC) than degradation. Likewise, the systems are expected to be more consistent in primary forests, where the loss of tree cover is more likely to be detected by both products. Both masks will be used in this study in order to compare systems in different forest mask with *primary forest mask* being a subset of the *undisturbed forest mask*.

Both forest extents were validated for the end of the year 2015 using the validation dataset produced by the Central African Forest Initiative (CAFI). This dataset is made of roughly 350.000 points of stable landcover upon which 180.000 (displayed in Figure 4A) can be labelled as “tropical moist forest”. Figure 4B detailed which CAFI land cover classes were considered as undisturbed tropical moist forest or not. Secondary forest was not considered as undisturbed tropical moist forest as they represent forest

that experienced noticeable degradation in the past and as such could not be considered as undisturbed anymore.

GLAD 2015 primary tropical moist forest mask was obtained by removing all pixel that encountered FD from GFC until 2015 included from the initial 2001 GLAD *Primary humid tropical forests mask*[29]. The JRC undisturbed tropical moist forest mask was extract for the year 2015 using the class 1 of the *Annual Change Collection*[30].

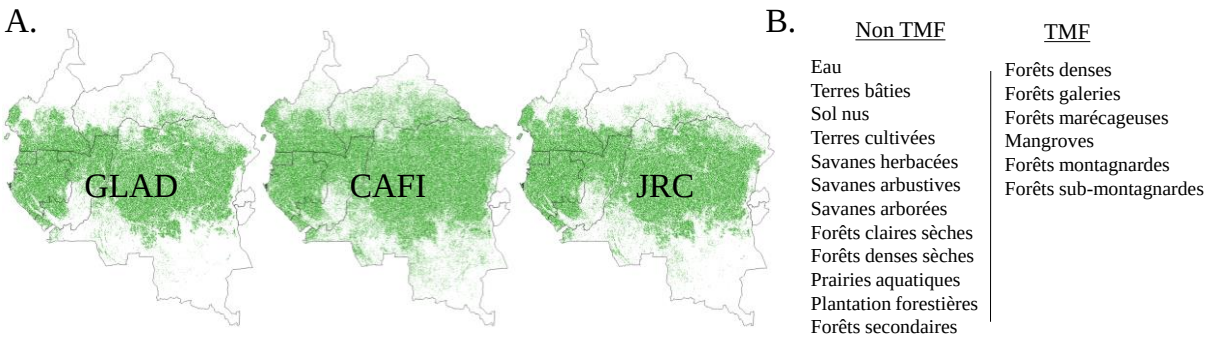

Figure 4: A. *Maps of validation points labelled as tropical moist forest (in green) according to GLAD's Primary Forest mask (left), according to CAFI (centre) and according to JRC's Undisturbed tropical moist forest mask. Non tropical moist forest points are in white.* ***B.*** *List of land cover names from the CAFI dataset belonging to TMF and Non TMF class in French.*

Validation results detailed in *Table 1* shows that both systems have similar performances for tropical moist forest mapping in regards with the CAFI dataset even if JRC mask performs slightly better than GLAD mask. *Table 1* also shows an important level of agreement between GLAD and JRC datasets suggesting that those masks are somehow similar in their overall extent. Figure 4A suggest that most of the disagreement between both forest mask and CAFI validation samples are located at the north and south edges of the Congo Bassin, were the distinction between tropical moist forest and other forest type is harder to determined due to climatic and floristic considerations.

Table 1 : *Confusion matrices between JRC dataset and CAFI (Left), between GLAD dataset and CAFI (Middle). The last matrix (Right) shows the important level of agreement between both masks. Orange cells are overall accuracies.*

		JRC undisturbed TMF mask		
		Prediction		
		Non TMF	TMF	Recall
True	Non TMF	150049	16726	0,90
	TMF	34470	148106	0,81
	Precision	0,81	0,90	0,85
	F-score	0,85	0,85	

		GLAD primary TMF mask		
		Prediction		
		Non TMF	TMF	Recall
True	Non TMF	154024	12751	0,92
	TMF	45039	137537	0,75
	Precision	0,77	0,92	0,83
	F-score	0,84	0,83	

		GLAD primary TMF mask		
		Non TMF	TMF	Recall
JRC	Non TMF	180706	3813	0,98
	TMF	18357	146475	0,89
	Precision	0,91	0,97	0,94
	F-score	0,94	0,93	

It should be noticed that this validation is only accurate for 2015 Central African tropical moist forest. However, considering the amount of stable land cover samples used and their random distribution across central Africa, it is assumed that this validation is still useful to evaluate the accuracy of those products to depict the tropical moist forest. *Table 2*, presenting accuracy metrics by countries, also suggest that JRC TMF mask outperform GLAD mask in every country. For both systems, recall statistics demonstrate that both systems severely underestimate the tropical moist forest cover in the Central African Republic. On the other hand, both systems misclassified the non-tropical moist forest class in Equatorial Guinea and to another extent in Gabon. With a recall of 0.77, GLAD mask significantly underestimates tropical moist forest extent in the DRC in comparison with JRC mask. *Table 2* shows also that Equatorial Guinea and Cameroun are the countries where forest masks disagree the most with each other. Finally, *Appendix 1* detailed the proportion of well classified pixel by land cover for each mask and the overall agreement between them for each land cover. This table shows that many minority classes like mangroves, mountainous forest, riparian forest, or water are the classes associated with the

[29] https://glad.umd.edu/dataset/primary-forest-humid-tropics
[30] https://forobs.jrc.ec.europa.eu/TMF/data.php

highest omission errors. More critical are the significant errors in the build-up and secondary forest classes for the JRC mask validation (below 70 % recall). The same table shows important level of agreement between GLAD and JRC masks for all land cover at exception of mangroves forest.

Table 2 : *Accuracy metrics by countries by class for each mask (from left to right: Precision, Recall, F-score, Overall Accuracy, number of CAFI samples in the country and percentage of CAFI samples in the country). The bottom table provide the overall agreement by countries between GLAD and JRC masks.*

	JRC undisturbed TMF mask								
	Recall		Precision		F-score				
	TMF	No TMF	TMF	No TMF	TMF	No TMF	OA	Samples	% samples
Gabon	0,96	0,53	0,92	0,72	0,94	0,61	0,90	23427	6,7
Equatorial Guinea	0,95	0,19	0,90	0,35	0,92	0,25	0,86	2440	0,7
Republic of the Congo	0,91	0,82	0,91	0,82	0,91	0,82	0,88	30015	8,6
Democratic Reublic of the Congo	0,82	0,90	0,90	0,82	0,86	0,86	0,86	202974	58,1
Central African Republic	0,35	0,97	0,83	0,78	0,50	0,86	0,78	52252	15,0
Cameroun	0,85	0,87	0,88	0,85	0,86	0,86	0,86	38243	10,9

	GFC primary TMF mask								
	Recall		Precision		F-score				
	TMF	No TMF	TMF	No TMF	TMF	No TMF	OA	Samples	% samples
Gabon	0,92	0,65	0,94	0,60	0,93	0,62	0,88	23427	6,7
Equatorial Guinea	0,84	0,34	0,90	0,22	0,87	0,26	0,78	2440	0,7
Republic of the Congo	0,85	0,87	0,93	0,75	0,89	0,81	0,86	30015	8,6
Democratic Reublic of the Congo	0,77	0,93	0,92	0,79	0,84	0,85	0,84	202974	58,1
Central African Republic	0,32	0,97	0,81	0,77	0,46	0,86	0,77	52252	15,0
Cameroun	0,75	0,92	0,90	0,77	0,82	0,84	0,78	38243	10,9

GLAD & JRC masks overall agreement					
Gabon	Equatorial Guinea	Republic of the Congo	Democratic Republic of the Congo	Central African Republic	Cameroun
0,94	0,86	0,93	0,94	0,96	0,86

The combination of qualitative and quantitative analysis allows to distinguish two forest masks that are semantically similar at first sight. It appears that the *Primary Forest mask* is more restrictive than the *Undisturbed Tropical Moist Forest mask* especially in degraded forest and the first might even be considered as a subset of the second. In this paper, both masks will be used as they represent two realities in terms of FD dynamics and forest definition. By subtracting the *Primary Forest mask* to the *Undisturbed Forest mask* we obtained a third forest extent representing forest areas located inside the *Undisturbed Forest mask* that were not considered as forest by the *Primary Forest mask* which represent rural complexes and sparse moist forests.

3.1.3 System intersection for a comparative analysis

GFC tree loss detections are compared with TMF's degradation year (DEG) and deforestation year (DEF) datasets. To keep a track of both spatial and temporal intersections, special encoding was performed for the products comparison at pixel level during the data combination. Data were then masked with the 2000 undisturbed TMF extent from the *Annual Change Collection* as presented in Figure 5. In a second step, the same data are masked using the *Primary Forest mask* from GLAD.

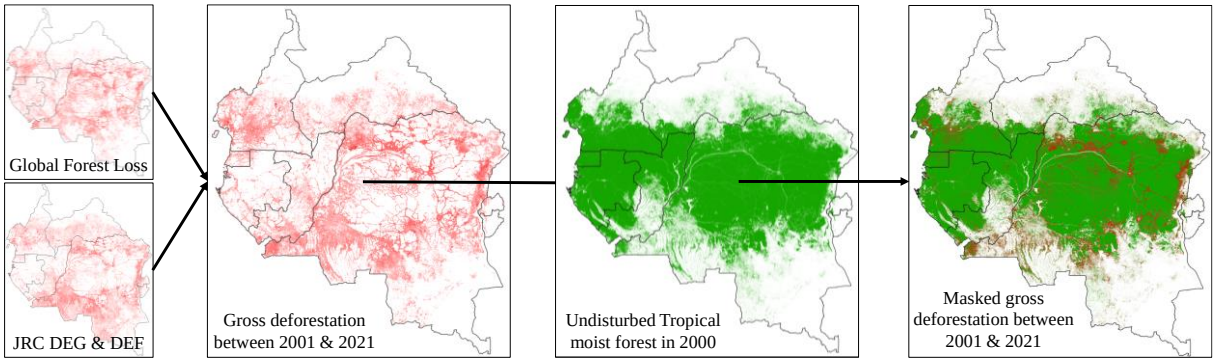

Figure 5: *Global Forest Loss data from GFC are combined with degradation (DEG) and deforestation (DEF) data coming from the TMF dataset. They are then masked with the 2000 undisturbed TMF extent. A large cubic resampling was performed on GFC and JRC maps displayed in this figure for visual purposes only.*

The pixel-based intersection between DEF, DEG and GFC datasets create seven mutually exclusive spatial intersection classes detailed in the Figure 6. Three classes (GFC, DEF and DEG) represent disturbance events only detected by one dataset. One class concerns the pixels that encountered degradation before deforestation (DEF∩DEG). Three classes show the intersection between GFC and either DEG or DEF or both (respectively DEF∩GFC, DEG∩GFC, GFC∩DEF∩DEG). From those three last classes, eleven temporal sub-classes can be defined depending on which dataset detect FD the first or if two datasets detected FD at the same time. Each class can be associated with a relative level of confidence in regards with the probability that a significant forest disturbance event actually happens depending on spatial, temporal and semantics considerations. The resulted intersection maps are presented in *Appendix 5* for each COMIFAC countries with the exception of Sao-Tomé et Principe which is not covered by any system and the Republic of Chad which is not covered by any tropical moist forest.

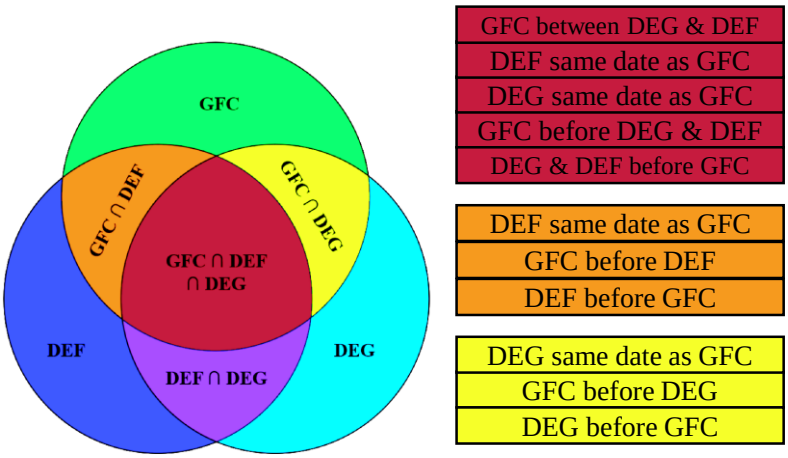

Figure 6: *Venn diagram showing the seven spatial intersection classes and the ten associated temporal sub-classes.*

3.2 Methodological analysis

3.2.1 Systems initial objectives

TMF products offers a consistent wall-to-wall mapping of tropical moist forest cover dynamics at the resolution of 30m. The extent of forest degradation and deforestation are for the first time dynamically quantified (Vancutsem et al., 2021). Deforestation is defined as the permanent conversion from moist forest to another land cover. Degradation is defined as a brief time period disturbance.

The GFC product aims to map the percentage of the world's tree cover in 2000 and the change in this cover over time at 30m resolution. Forest is defined here as land cover with a vegetation canopy higher than 5m, regardless of the initial 2000 canopy cover percentage (from 1 to 100% of a Landsat pixel). Deforestation is defined as a total loss of tree cover considered as the complete conversion of a forest to another land use. This product is not specific to dense rainforests and does not consider degradation dynamics as separate events. With such straightforward and basic definitions, the GFC product is on paper fully comparable with other deforestation detection products, as long as a common detection forest mask is applied.

On the other hand, TMF aims to map dynamics of more complex changes in tropical rainforests. The dynamics to consider in here are deforestation, which is the permanent conversion of a dense tropical moist forest into another land cover and degradation which is defined as a low intensity disturbance of the observed canopy over a brief period of time. The intensity of a disturbance is calculated on an annual scale by analysing the ratio between the number of disturbances detected in a year and the number of valid observations available in that same year. If the ratio value is less than 0.45 then the pixel is labelled as degradation (0.23 if the first disturbance is detected in the second half of the year). Conversely, if these thresholds are exceeded, the pixel will be labelled as direct deforestation. The inter-annual aggregation is used to differentiate occasional disturbances (less than 2.5 consecutive years) from a longer disturbance associated with a slow process of deforestation (more than 2.5 consecutive years) leading to land use change. TMF does not consider any tree cover or tree height reference in their forest definitions but mentioned that all closed canopy forest in the humid tropical domain is the target of the system.

We see here that the differences in objectives are important both in the domain of detection (TMF operating in a much more restrictive area than GFC) and in the definition of key concepts; however, the choice of a common forest mask and detection period allows to overcome some discrepancies. An analysis of the system’s goal shows that TMF will produce significantly more disturbances than GFC by the mere consideration of degradation processes. It might be tempting to use only detections labelled as deforestation by the TMF system for the comparison with GFC detections, but it is forgotten that in wet tropical environments, regrowth processes are fast and valid optical satellite data are scarce. As a result, it is likely that some pixels experiencing a total loss of tree cover will still be labelled only as forest degradation by TMF without being labelled as deforestation in the following years. Therefore, a conservative approach considering DEF and DEG should lead to more comprehensive comparison results.

3.2.2 Algorithms strengths and caveats

Even if the same input data is used for change detection in both systems, the applied algorithms are completely different and confront two different paradigms for change detection: time series analysis for GFC and post-classification change detection based on single-acquisition classification for TMF.

The method used by TMF involves predicting for each valid observation of the object to be monitored (in this case a Landsat pixel) whether or not it belongs to a class of interest (dense rainforest or non-dense rainforest). This wall-to-wall mapping method does not really detect changes in land cover per se, but rather maps the extent of dense rainforest for each acquisition. Such a method applied over a long

time series inevitably generates cumulated commission errors if a total dependence is not observed between successive classifications. However, this post-classification change detection method is strongly consolidated by a series of intra- and inter-annual aggregations of the classifications results that allow differentiation between short degradation, direct deforestation, and deforestation after degradation (using the previously mentioned expert-based threshold numbers which are 0.23, 0.45 and 2.5 years). This consolidation is further strengthened by the existence of a post-classification of degradation types between those describing a one-off low-intensity event and those observed on a more recurrent basis. This consolidation, combined with the probable strong dependence of those successive classifications due to the use of same input data and models, means that commission errors are expected to be low and will mainly be located within the degradation classes. This same method also guarantees a low rate of errors of omission, as even truly short, low-intensity changes will be recorded in the database.

In regions were cloud free data are mainly taken at the beginning of the year, it is unlikely that a TMF detection might be labelled as "Deforestation", as there is never enough observation after the disturbance event in order to overcome the 0.45 and 0.23 thresholds. This issue is expected to increase with the addition of new optical data-sources as month with low cloud coverage will be over-represented in the annual dataset. If this unbalanced dataset is in favour of the beginning of the year, the number of new TMF detection labelled as deforestation decrease as the number of valid optical observation increase. This affirmation is highlight in Figure 6. Here, the probability of having a weekly cloud-free composite of SPOT data (Lamarche et al., 2014) is use as a proxy of the probability of having a cloud-free optical observations in general with a daily revisit. If we use those probability with the 0.45 and 0.23 TMF thresholds, we can plot the month from with a complete and long-lasting clear cut (every valid detection is well classified as tropical moist forest or not by TMF) will be classified as a degradation regardless of the perturbation intensity. In regions where cloud coverage is consistent, there is only an issue with the perturbation detected at the end of the year, in regions where there is a strong difference in cloud coverage between the end and the beginning of the year (such as the gulf of Guinea region), hardly any perturbation will be detected as a deforestation TMF. The Figure 6 presented the best scenario for TMF in which every valid observation acquired with a daily revisit led to a perfect discrimination between a tropical moist forest and a non-tropical moist forest. Considering that a deforestation is also a seasonal process (Gou et al., 2022) and that TMF intra-annual classification might sometimes be inaccurate, the misclassification of degradation and deforestation at a yearly basis might increase.

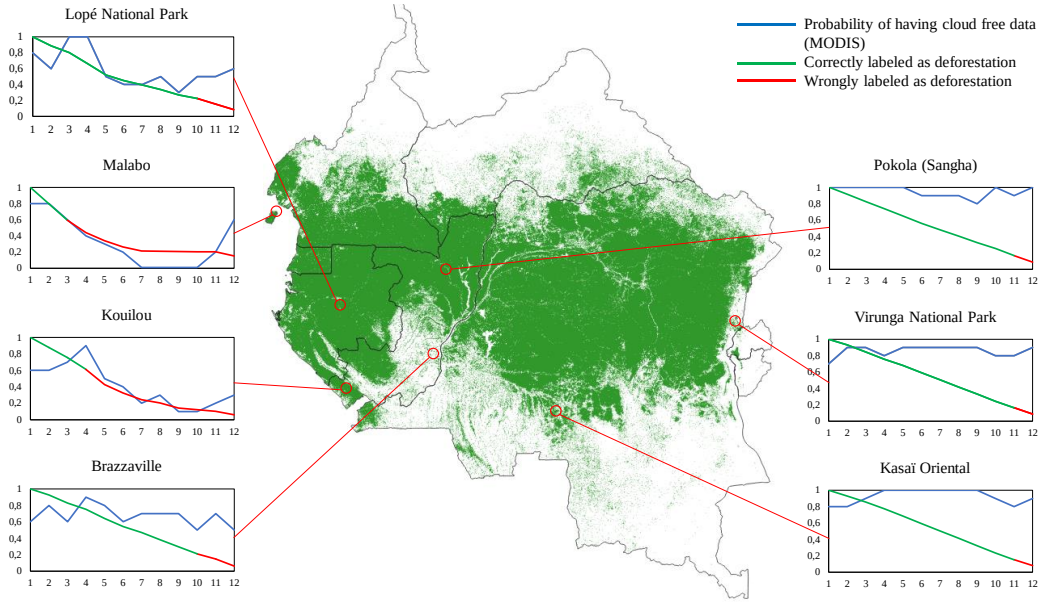

Figure 6 : *Monthly average of weekly probabilities composites of having cloud free images in various region of the Congo Bassin tropical moist forest (2001 TMF extent in green). The green and red curve represents respectively the period where TMF detections could be correctly and wrongly labelled as deforestation regardless of the intensity of the perturbation on an annual basis due to the interplay between clouds, valid observation frequency and TMF consolidation process.*

On the other hand, GFC chose a more conventional multispectral time series analysis as its primary tool for change detection. Using percentile and linear regression slope metrics, GFC allows its bagged decision tree to be stable and transferable in various detection domain producing consistent results in space and time. However, features were computed using growing season data only which induce a difference in image density for change detection between the forest located at the edges of the tropical rain forest domain (also including mountainous forest) and the forest situated in the heart of this climatic domain as the first experienced a much shorter growing season than the last. The perturbation initial start date is defined using the year of the maximum decline in NDVI during the growing season and the maximal annual decline in percent tree cover. Using this method for deforestation date assignment could generate some discrepancies with TMF as the last is way more sensitive than GFC, especially for long lasting degradation processes leading to a deforestation. The GFC methodology tends to produce strong reliable results in various detection domains minimizing commission errors but at the cost of important omission errors in the case of more complex or recurrent perturbation events.

The two radically different approaches of those systems produce results just as radically different depending on the types of perturbation a user is looking to monitor. GFC is expected to produce reliable detection for intense perturbation with low commission errors while TMF should detect every change happening in the moist forest domain even if it does not lead to deforestation or degradation processes thus containing much more commission errors in their dataset.

3.2.3 Conclusion of the methodological analysis

The methodological analysis already highlighted many potential sources of discrepancies and convergence between both datasets. The understanding of their objectives, algorithms, and detection domains allows us to redefine the expected nature of each dataset.

- **GFC** masked with the undisturbed tropical forest extent: precise detections of tree cover loss regardless of the event's duration, the initial tree cover, or the previous degradation processes.
- **Deforestation** dataset from TMF: exhaustive yet not precise detection of either an intense disturbance event or an at least 2.5 years old continuous degradation process.
- **Degradation** dataset from TMF: exhaustive detection of either short disturbance event or long-lasting discontinuous degradation processes. This dataset is where most of the false detection is expected to arise. In some cases, when data are scarce, or regrowth is particularly fast, complete but not permanent stand-replacement can also be labelled as degradation.

It should be noticed that for the last three years of the TMF dataset, the distinction between degradation and deforestation is a bit blurry because of the consolidation procedure.

This analysis only refers to methodological considerations. The following pages will use ancillary data, datasets intersections, as well as geographical and temporal consideration to provide better understanding of GFC and TMF datasets.

3.4 Regional patterns and national performance variability

The GFC forest monitoring system reports a forest disturbance extent of 7,44 Mha while the TMF system detect 10,5 Mha for the same primary forest mask, with a spatial correspondence of 6,24 Mha. However, the TMF monitoring system using its own undisturbed tropical forest mask reports a total forest disturbance extent of 28,53 Mha, four times higher than GFC, made of 11,60 Mha of deforestation (DEF) and 16,93 Mha of forest degradation (DEG).

Maps and statistics of Figure 8 showed that the TMF system detected a much larger number of perturbations than GFC in both undisturbed and primary forest masks. Indeed, only 47% of the TMF detection are also detected by GFC while considering DEF and DEG detection in the undisturbed tropical forest mask. This system convergence is not higher than 53% using the primary forest mask and drops to 24 % when only considering the DEF class from TMF rather than DEG and DEF classes.

At the opposite, this pixel-based wall-to-wall analysis indicates that most of GFC detection are also detected by TMF. In the undisturbed forest mask, 88% of GFC detections (13.31 Mha out of the 15.13 Mha FD detected by GFC) were also detected by TMF. In the primary forest mask, the situation is similar with 84% of GFC detections (6.24 Mha from the 7.44 Mha of FD detected by GFC) also detected by TMF.

This can be partly explained by the fact that about two-third of the total amount of GFC and TMF detections are located outside of the primary forest mask, hampering GFC to detect any disturbance in this area. Figure 7 shows that this proportion is even higher in exclusive TMF detections and in particular for the DEG∩DEF class. Obviously GFC and TMF shows higher agreement in the primary forest mask than in the undisturbed forest mask.

Strong differences in the proportion of intersection classes are observed between countries in primary and non-primary forest mask (Figure 7 and Appendix 5). A clear dichotomy between regions on the periphery and regions in the center of the equatorial zone is visible on the map below (Figure 7). Formers have a much higher proportion of disagreement in favor of TMF than the latter within undisturbed forest mask. This dichotomy is less marked at country level and within primary forests, although the BDI, RWD and CAR clearly stand out from the other countries.

This analysis quantitatively and qualitatively confirms previous statements about the impact of algorithm design and product goals on their actual detection performances producing distinctive regional patterns. Those statements being the predictable higher amount of detection produce by TMF in every forest mask, higher agreement between both systems in primary forest and the predominance of TMF detections at the periphery of the hot humid climatic region, where seasonal effects are more important than in the equatorial zone. The divergences between countries might also be explained by the fact that forest dynamics are mostly driven by the cropland expansion in the DRC, CAR and CMR, compared with other logging activities, more prevalent in Gabon (Tyukavina et al., 2018).

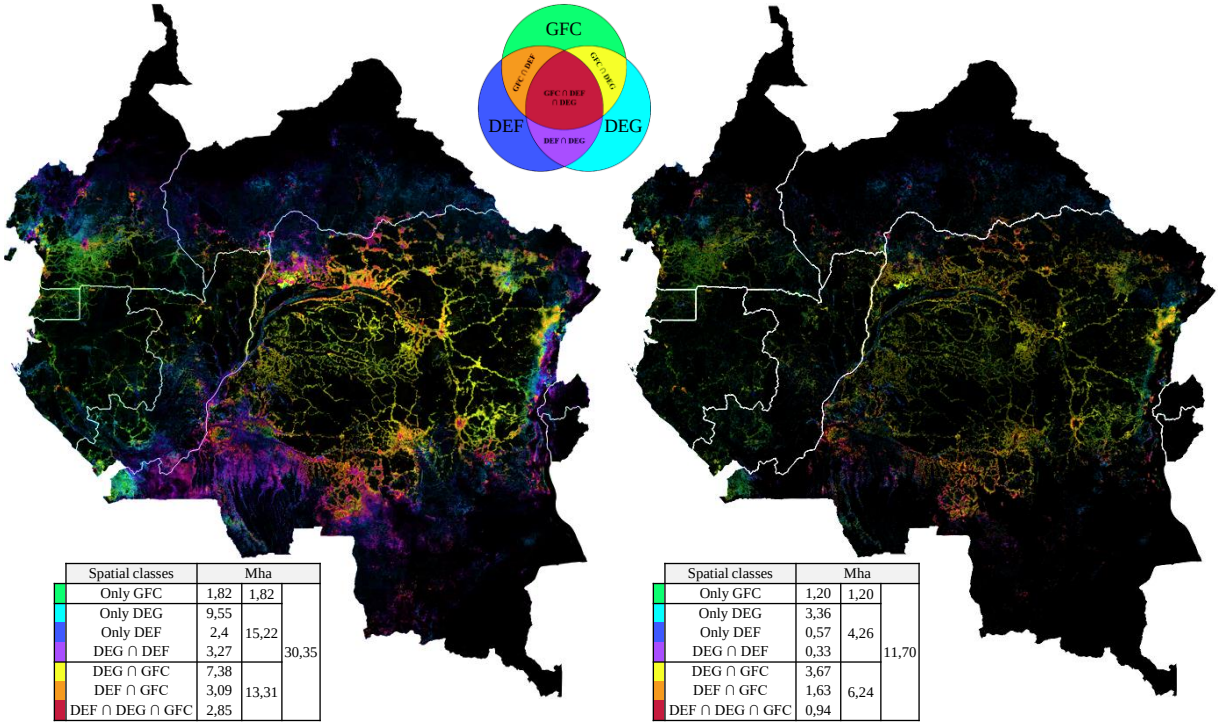

Spatial classes	Mha		
Only GFC	1,82	1,82	
Only DEG	9,55		
Only DEF	2,4	15,22	
DEG ∩ DEF	3,27		30,35
DEG ∩ GFC	7,38		
DEF ∩ GFC	3,09	13,31	
DEF ∩ DEG ∩ GFC	2,85		

Spatial classes	Mha		
Only GFC	1,20	1,20	
Only DEG	3,36		
Only DEF	0,57	4,26	
DEG ∩ DEF	0,33		11,70
DEG ∩ GFC	3,67		
DEF ∩ GFC	1,63	6,24	
DEF ∩ DEG ∩ GFC	0,94		

Figure 7: Intersection map between TMF and GFC dataset from 2001 to 2021 within Undisturbed tropical moist forest (left). Intersection map between TMF and GFC dataset from 2002 to 2021 within Primary tropical moist forest (right)**.** High cubic resampling on colors is applied for visualisation purposes only, but not for area estimation statistics.

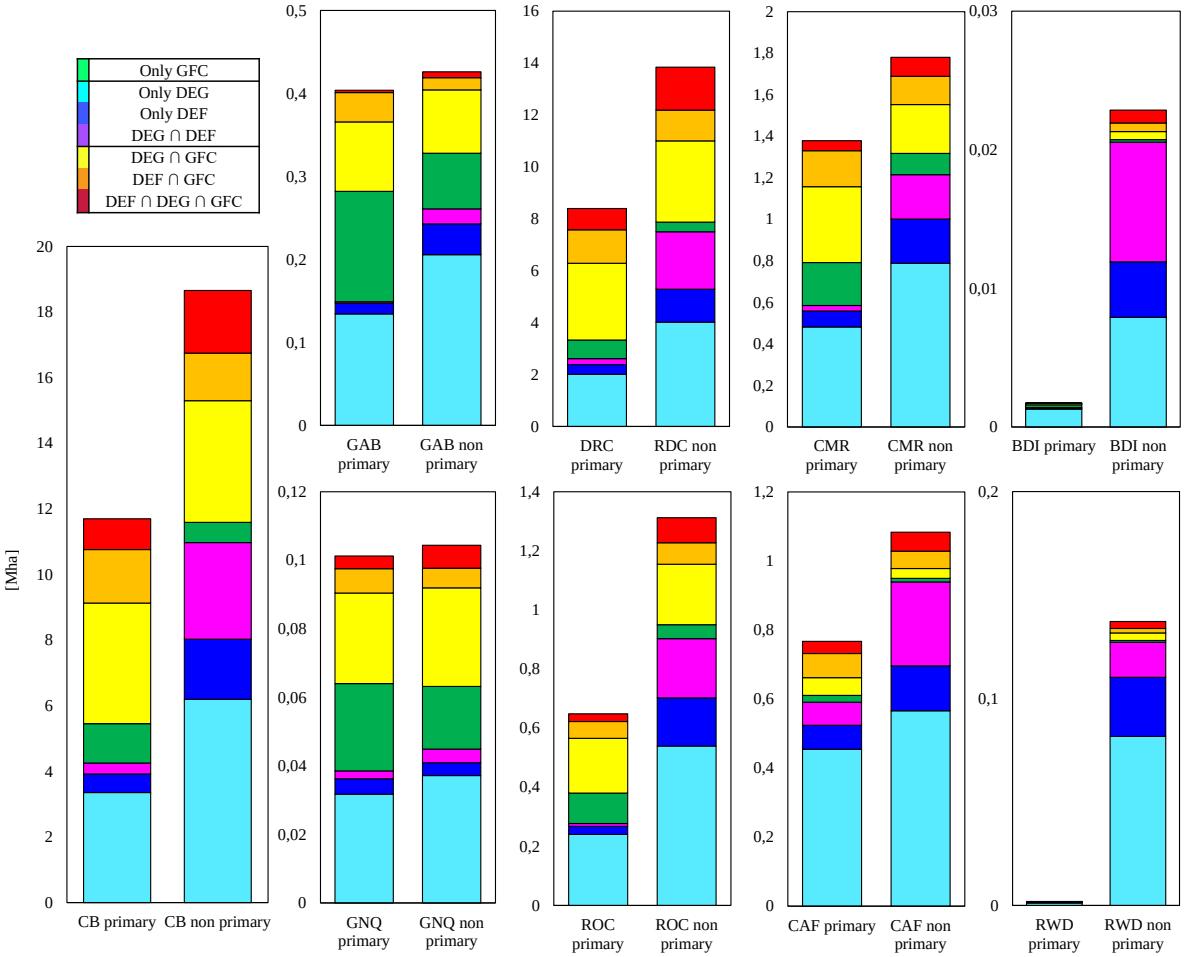

Figure 8: *Surface covered by each intersection classes for each country and for the Congo Bassin region (CB) for primary and non-primary forest. The same information in proportion of the total number of national detections are also presented in* ***Appendix 2.***

3.5 System's agreement in time and long-term deforestation trend

Population demography, socio-economic condition evolution, land use planning policies, climate change, intensification of the rural exodus, but also the increase in Landsat data available are many factors that can influence the performance of both systems over time. In order to analyse the detection timeliness of both systems, the annual change as new detections has been calculated for the three forest masks. Each new detection is dated and labelled according to the first system detecting the FD. As a result, the DEG∩DEF and DEG∩DEF∩GFC classes do not exist in this analysis. However, GFC∩DEG and GFC∩DEF classes exist if both systems detected the FD in the same year. The annual evolution of new disturbance detections is depicted in Figure 9.

Figure 9.3 shows that the annual number of new disturbances tends to increase over time in primary forests, whereas it tends to decrease in non-primary forests, resulting in stagnation in undisturbed forests. These findings can be explained by the irreversible nature of the detections considered here. As regrowth is not considered in this study, the area of non-primary forest in 2000 within which it is possible to detect disturbances becomes smaller every year as disturbances are detected. As this area is fairly limited relative to the *primary forest mask* area, it is normal to see fewer and fewer detections as the whole domain is at least cut once. Figure 9.3 also shows that primary forest is increasingly disturbed. Figure 9.1 shows that degradation detection are the predominant dynamics across time. The year 2013 start a period of higher number of detections, this is mainly explained by the launch of Landsat 8. This period peaks at the year 2016 due to abnormal fire events happening across the whole region due to a major

drought caused by strong El-Nino event. As such, long term dynamics analysis should not use the 2013-2016 period as an indicator of systematic increase of deforestation in the Congo Bassin area. Figure 9.2 demonstrate that the yearly agreement between systems is increasing over time reaching an all-time high in 2021 where 50% of the annual perturbations are detected in the same place at the same time by both datasets. This convergence is found in the three forests mask but is stronger under *the primary forest mask*. The convergence might be explained by the fact that new detections are more and more likely to be located within dense primary forest where the agreement between systems is the highest as well as because of even improving Landsat image quality and quantity.

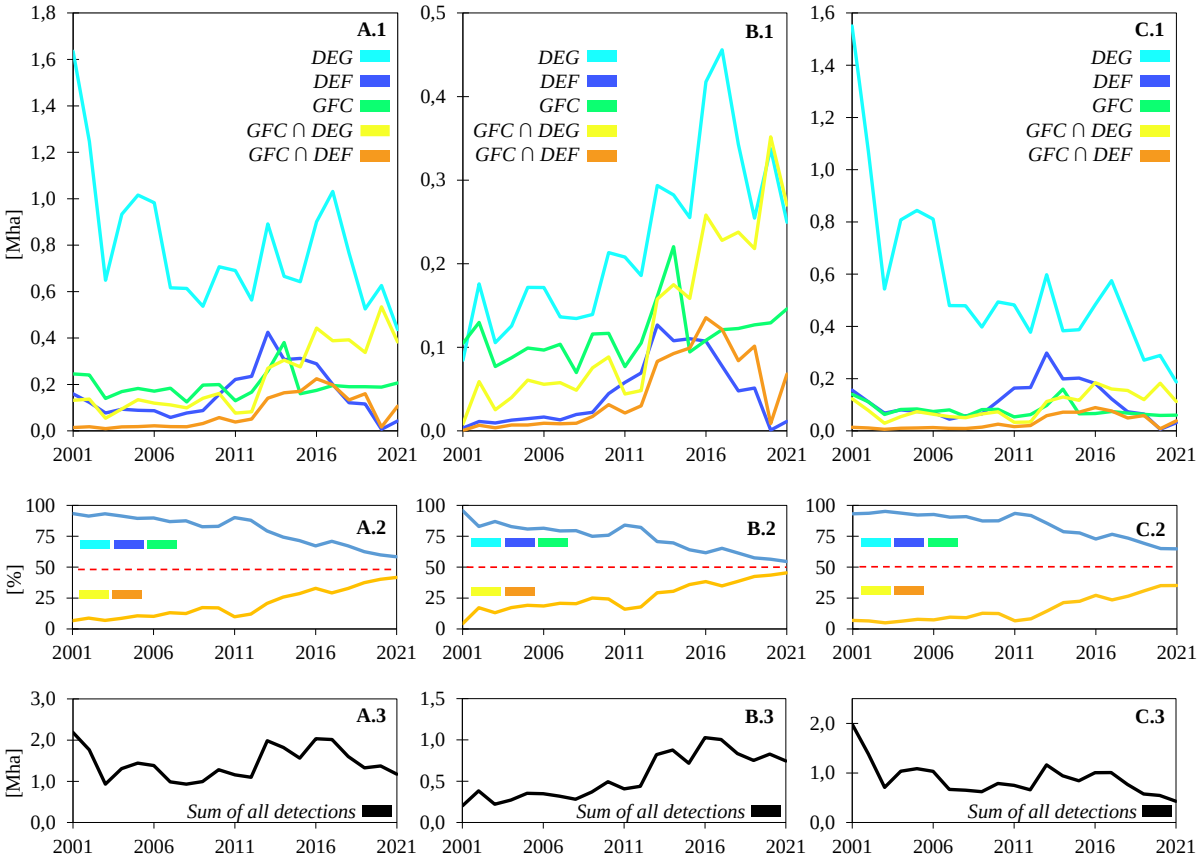

Figure 9: *Annual evolution of new disturbance detections in* ***A.*** *undisturbed forests (TMF masks),* ***B),*** *primary forests (TMF mask ∩ Primary Forest mask) and,* ***C.*** *non-primary forests (outside the TMF ∩ Primary Forest mask) in the Congo Basin. The figure shows* ***1.*** *the evolution of the detections for the 5 classes of intersection possible for a first detection (GFC ∩ DEF and GFC ∩ DEG representing the intersections detected at the same time by GFC and TMF),* ***2.*** *the progressive convergence showing both systems more and more in agreement with each other for the detection of new perturbations (in Blue the sum of the classes DEG, DEF and GFC, i.e. the classes that did not find new perturbations at the same time, and in Orange the sum of the classes GFC ∩ DEF and GFC ∩ DEG, i.e. the classes that found new perturbations at the same time) and* ***3.*** *the sum of all new perturbations decomposed into* ***1.****.*

Figure 10.A shows the distribution of detections spatially common to GFC and TMF, aggregated over the period 2001-2021 within undisturbed forests, as a function of the time lag between these common detections. Analysis of the results shows that half of the disturbances common to the two systems spatially are also common temporally. If an error of +- 1 years is allowed in view of the system specifications, this figure rises to over 60%. Figure 10.B depicted the same data for primary forest extent, the distribution is even more centred around a 0 +-1 year delay, representing 70% of the spatially common detections. In conclusion, when systems agreed on the location of disturbances, they also agreed on the year of this disturbance, and this tends to improve over time. This growing convergence of systems is mainly caused by the progressive increase in the volume of data available, allowing a more conservative system like GFC to generate audacious predictions than before. Indeed, denser time series make it possible to calculate finer metrics and thus reduce the number of omissions without reducing

commission errors. It can be said that the GFC system, through its algorithm, has the power to adapt to the data availability. Conversely, the increase in valid observations is pushing TMF to label its detections as degradation. As disturbance events are often followed by significant regrowth in the Congo Basin, and even more so in primary forests, the ratio of "annual disturbances/annual valid observations decrease a lot and often prevent disturbances from being labelled as deforestation. This also explains the sudden increase in new perturbations labelled as GFC ∩ DEG after the launch of Landsat 8.

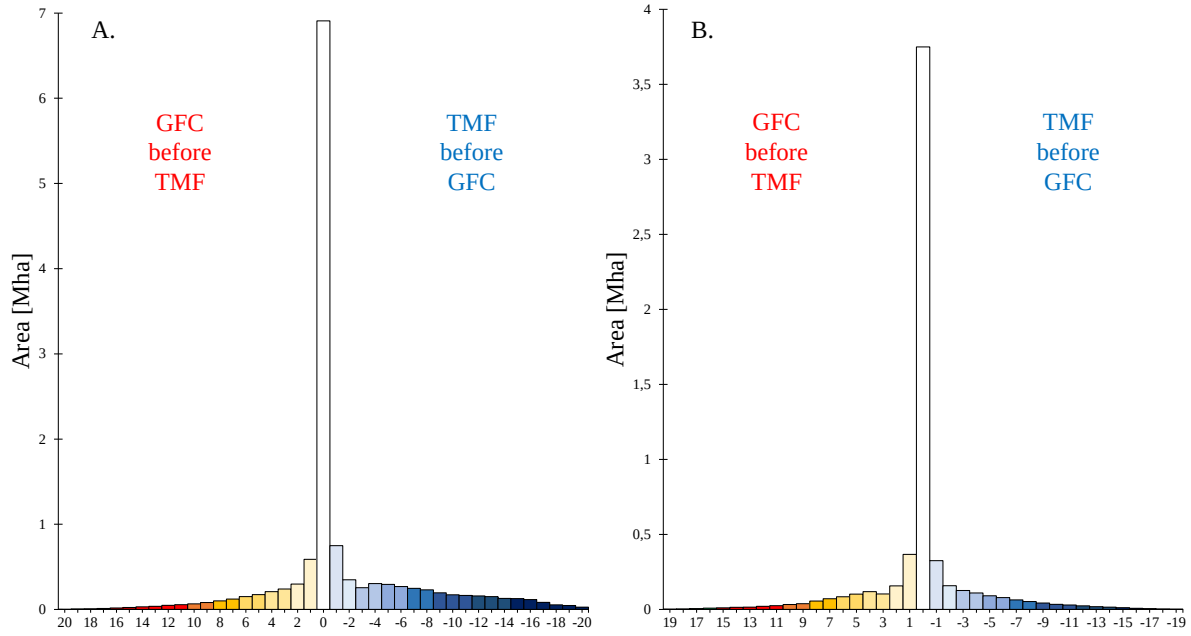

Figure 10: Distribution of the delay (in years) between GFC and TMF when they detect perturbation at the same place. Positive years means that GFC detect a perturbation before TMF and Negative years means that TMF detect a perturbation before GFC. **A.** for undisturbed forest and **B.** for primary forest.

3.6 Relation between systems and forest definitions

In order to better understand the differences between the systems, it was decided to analyse the relationship between intersection types with the tree cover and canopy height variables that is often used to define a forest. Both information are provided at 30m resolution by the UMD.

3.6.1 Tree cover

Figure 11 shows the cumulative and disaggregated distribution of intersection types according to the percentage of tree cover in 2000 for all disturbances detected between 2001 and 2021. We assume that stable tropical moist forests does not change significantly in tree cover percentage over time and when those forest experienced a significant tree cover loss, it would be detected by either of the systems. Given the “dense” property of tropical moist forest, an asymmetric distribution in favour of high tree cover value is expected. This is observed for most intersection types at the exception of DEG∩DEF and only DEF classes. These exceptions indicates that most of the detections belonging to those classes refers to perturbation events happening at the edges of what is commonly considered as tropical moist forest.

The same distributions are shown in Appendix 3 and 4 for *primary forests and non-primary forest mask* (i.e., rural complex, or heavily degraded forests). Analysis of these three figures provides a better understanding of the nature of the detections occurring in the different forest masks and within the various intersection classes. Detections within primary forests mainly concern dense forests (asymmetric distribution for all intersection classes), in contrast to those located in non-primary forests (systematic flattening of distributions towards less dense cover). Note that even within non-primary forests, the GFC and GFC∩DEG classes maintain an asymmetric distribution.

The distribution of the DEG class represent the wide variety of disturbances not leading to deforestation (occasional degradation, degradation at the edge of deforested areas, small-scale timber harvesting, ...) and often taking place within highly degraded forests with less dense canopies. The situation of DEF and DEG∩DEF classes is more critical as they represent high intensity disturbances or at least long duration disturbance. The fact that they have not been detected by GFC and that they mainly concern sparse forests within an already degraded landscape makes them rather doubtful or unexpected for a tropical moist forest monitoring system, especially in the non-primary forest mask. In fact, those two classes often do not fit TMF forest definition claiming to monitor only closed canopy forest.

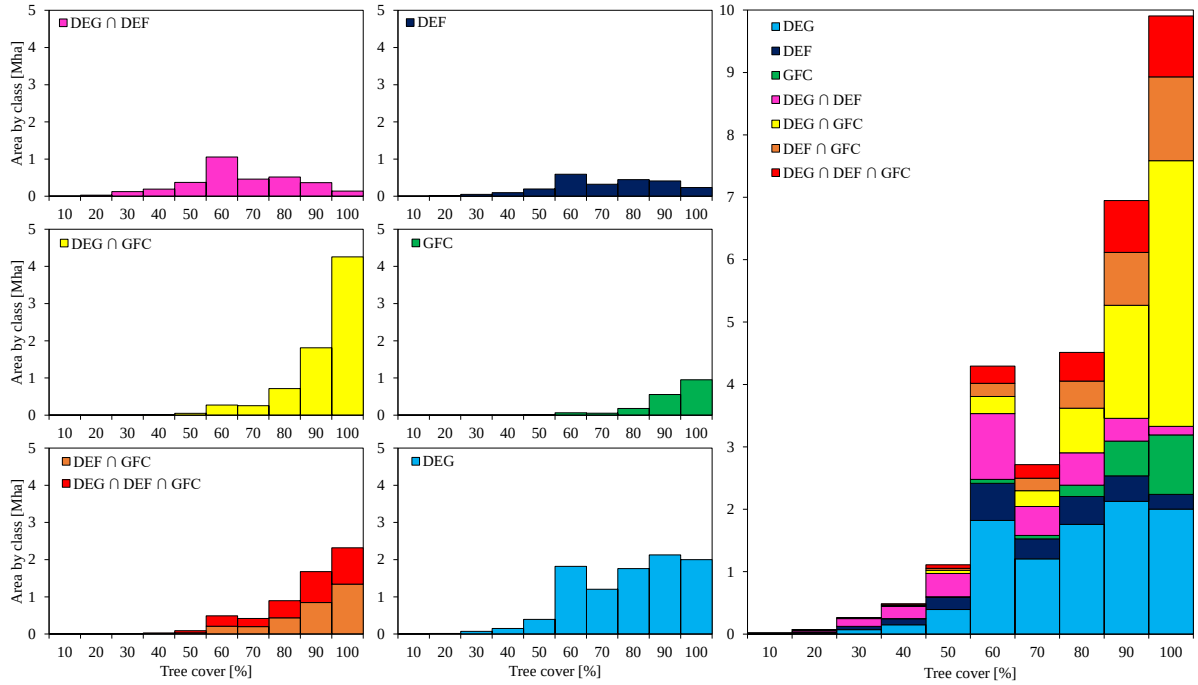

Figure 11: *Disaggregated distributions of intersection types according to the percentage of tree cover in 2000 for all disturbances detected between 2001 and 2021 within undisturbed tropical moist forest mask.*

3.6.2 Canopy height

The 30m resolution canopy height can be obtained using the *Global Forest Canopy Height* product. This dataset is available for the year 2019 use the Global Ecosystem Dynamics Investigation (GEDI) valid data as calibration and Landsat time series from April to October 2019 (Potapov et al., 2020). This product is not without uncertainties and the model used tends to saturate above 30m. However, it can still be used to further analyse the intersection classes.

Tree growth in the dense, moist forests of central Africa is rather fast. Trees such as the *Musanga ceratioids* can reach growth rates of several metres per year, potentially reaching 15m in 9 years, before gradually giving way to slower growing trees (World Agroforestry, 2018). However, after a clear cut, it takes several decades to reach a mature canopy height of over 20m height. By cross-comparison of the 2019 canopy height data with deforestation data (combining all new detections from TMF and GFC for each year between 2001 and 2018 inclusive), canopy evolution after disturbance can be confirmed or not.

Figure 12 shows the canopy height in 2019 as a function of the year of disturbance. For example, of all the disturbances detected in 2003 in the Congo Bassin by GFC or/and TMF, 20% had a canopy height of less than 5 m in 2019, 47% less than 10 m in 2019, and so on. Analysis of the Figure 12 for 2017 and 2018 leads to the conclusion that a significant proportion of detections during this period are suspicious. It seems rather unrealistic that only one or two years after a disturbance, the canopy height is already above 15m. This situation applies to about 45% of the detections during this period. Although the canopy

height product has a vertical uncertainty, it is not significant enough to justify such a distribution of canopy heights. Selective logging of the tallest trees or the persistence of a degraded canopy within the rural complex may explain why a certain canopy height remains after the disturbance. The same analysis made for the 2001 to 2015 period shows a more expected distribution of canopy heights. Indeed, it is not uncommon for natural regeneration and canopy closure to restore canopy heights above 20m after 5 to 20 years of regrowth, although the presence of trees over 25m just 5 years after disturbance casts doubt on the accuracy/relevance of certain detections and/or the quality of the height product.

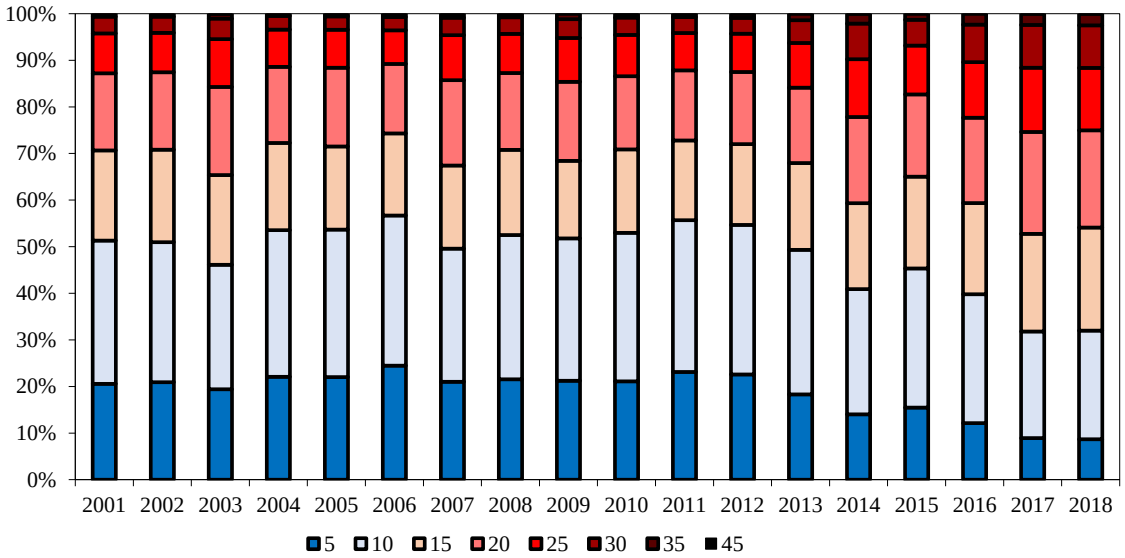

Figure 12:*Distribution of forest canopy height (color legend in meters) as a function of the date of the first disturbance between 2001 and 2018 in undisturbed tropical moist forest, as detected by TMF and/or GFC.*

Figure 13 shows the distribution of 2019 canopy heights for all pixels that experienced disturbance that happened between 2001 and 2018 aggregated by intersection classes. As a disturbed forest generally has an equally disturbed canopy, it is expected that the canopy height distribution will be asymmetric, with a majority of low values. This distribution is observed for the DEF and DEF ∩ GFC classes, but not for the GFC and DEG ∩ GFC classes. This can be explained by the fact that these last two intersection classes are often involved in disturbances located at the edges of rural complexes or in the heart of primary rainforest. In these areas, logging and small-scale farming activities are less intense and allow the canopy surrounding the cleared areas to quickly fill the gap. In contrast, the DEF and DEF ∩ GFC classes are most often found within new forest plantations or in the heart of rural complexes, i.e., where forest have limited regrowth capabilities or where forest are already composed of short trees. Another explanation could be that those detections are commission errors. As such, the high canopy of 2019 is more or less the same as the canopy height in the detection year because the canopy was never cut.

Assuming the quality of the canopy height products, the DEG detection follows an asymmetric distribution maintaining higher canopies than the DEF detection as expected. Contrarily, GFC seems to also maintain much higher canopy than DEF detections.

Figure 14 shows the canopy height data for 2019 with the sum of the new detections that occurred in 2020 and 2021 and disaggregate these detections by the five intersection types and by canopy height. The canopy height before the disturbance is presented for each intersection class. We can see that the DEG class, and especially the DEF class, concentrates detections that occurred in lower forest than the other three intersection types. This seems to confirm that DEF and DEG detections concentrate losses in sparsely wooded areas.

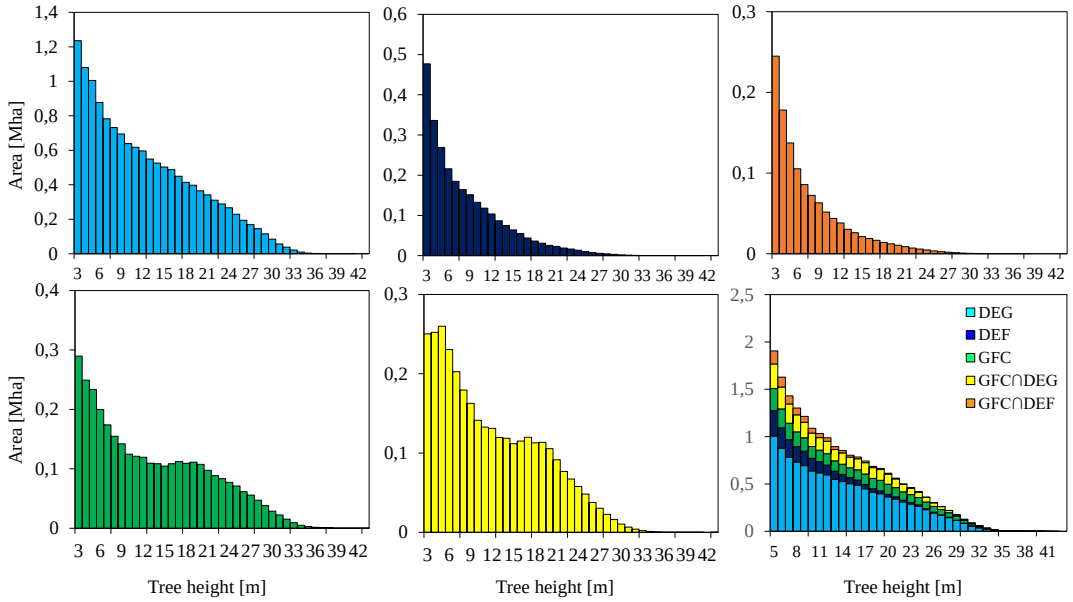

Figure 13: *Distribution of 2019 canopy height for each new detection between 2001and 2018.*

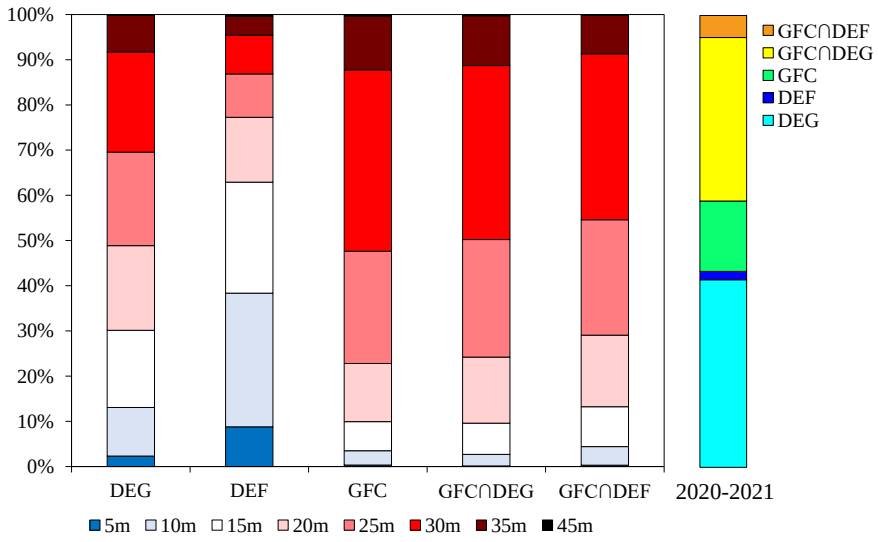

Figure 14: *Disaggregation of the different intersection types by canopy height (10m = canopy smaller than 10m). Here, only new perturbations are considered (on the left). Proportion of each intersection classes on the total amount of new perturbations detected from 2020 and 2021.*

In conclusion, tree cover and canopy height information partially indicates that GFC and TMF products contains doubtful detections or, at best, detections that occurred in dense tropical moist forest that do not fit with most definitions. Anomalies in tree height and tree cover highlighted with this analysis suggest large scale classification errors in every type of product intersection classes but especially inside DEG, DEG ∩ DEF and DEF classes. Tree height analysis also suggest that the DEG and GFC ∩ DEG class do not only represent short or/and low intensity disturbances. Similarly, the GFC detection distribution showing very high canopy is also rather unexpected.

3.7 System detection in various landscapes/land uses

Quantitative and qualitative analysis of the intersection maps highlights regional and local impact of some landscapes and land uses in the system's discrepancies or convergence which might indicates that both systems have specific sensitivity when it comes to the context of the deforestation and its drivers.

3.7.1 Water bodies and swamps

Visual analysis reveals areas of strong divergence located around rivers and swamps. Those areas are located all over Central Africa in a very caricatural way illustrated in Figure 15.

The TMF product has a disturbance subclass dedicated to deforestation caused by water. These sub-classes, illustrated in Figure 15 include disturbances caused by the filling of dams and those caused by the natural movement of the major rivers, notably the Congo, Kasai, Ogooué and Sangha. Although this layer seems visually correct for the two previous cases, it does not consider the disturbances caused by the frequent changes in edaphic conditions along these rivers. The natural movement of the river combined with extreme climatic events, such as the strong El Niño phenomenon of 2016, lead to changes in land cover that are sometimes intense, such as the drying out of swamp forests, making them more vulnerable to fire, or the conversion of these forests to aquatic grasslands. Those perturbations occur in every forest mask.

Although these disturbances do not represent a significant fraction of the total number of detections in the Basin and are generally located away from the major deforestation fronts, they can sometimes be significant in certain areas. It should be noted that these disturbances are mainly detected by the TMF product, whereas they are generally ignored by GFC, with the exception of those involving forest fires. Swamp forests, because of their fluctuating edaphic situation and their less dense nature than the other forests in the region, make it difficult to detect the presence of disturbances using time series metrics based on change slopes and percentiles like GFC. As GFC depict only change and not forest extent, most of the perturbation occurring within flooded forest are not detected. More critical is the inability to detect deforestation caused by river dams which correspond to clear cutting. As such, special attention should be paid when using GFC products in flooded forest and along dynamic water bodies.

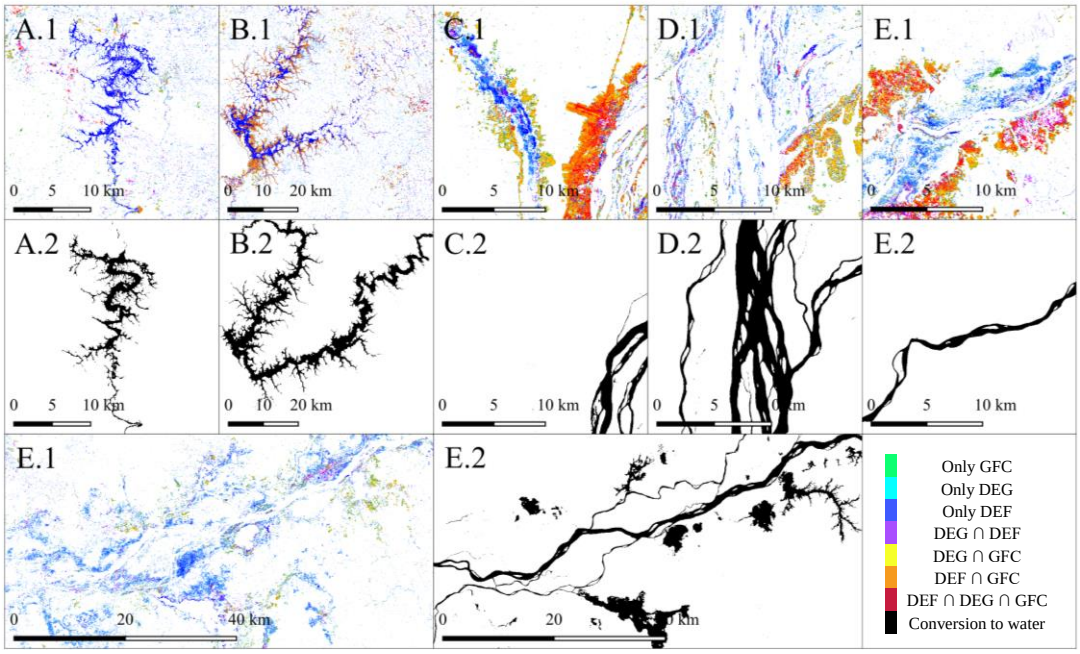

Figure 15: *Products behaviours around water bodies.* ***1.*** *The intersection map and* ***2.*** *the "Conversion to water" sub-classification (Permanent water, seasonal water, Conversion to seasonal water and Conversion to seasonal water) in black.* ***A.*** *Poubara dam in Gabon,* ***B.*** *Lom-Pangar dam in Cameroun,* ***C.*** *flooded Forest near Ibenga (Republic of the Congo),* ***D.*** *island and riverside of the Congo River near Lulonga (DRC) and* ***E.*** *Ogooué marshy delta in Gabon.*

3.7.2 Industrial plantation

Industrial plantations offers one of the best deforestation cases for both systems as they usually imply large scale clear cutting. As illustrated in Figure 16, new plantations detections usually show high agreement between systems (even if both systems are required to fully delimitate the plantation extent).

Complementary and convergent behaviours is limited to new plantations, as old plantations lead to poor intersection between systems. An “industrial plantation” sub-class proposed by TMF allows the segregation between old and new plantations. The important level of disagreement observed in those old plantations might be due to the high complexity of canopy dynamics within industrial plantation. The low omission error algorithm used by TMF allows the monitoring of those plantations in areas where data are sufficient, where the rare industrial plantation dynamics are not considered by GFC algorithms.

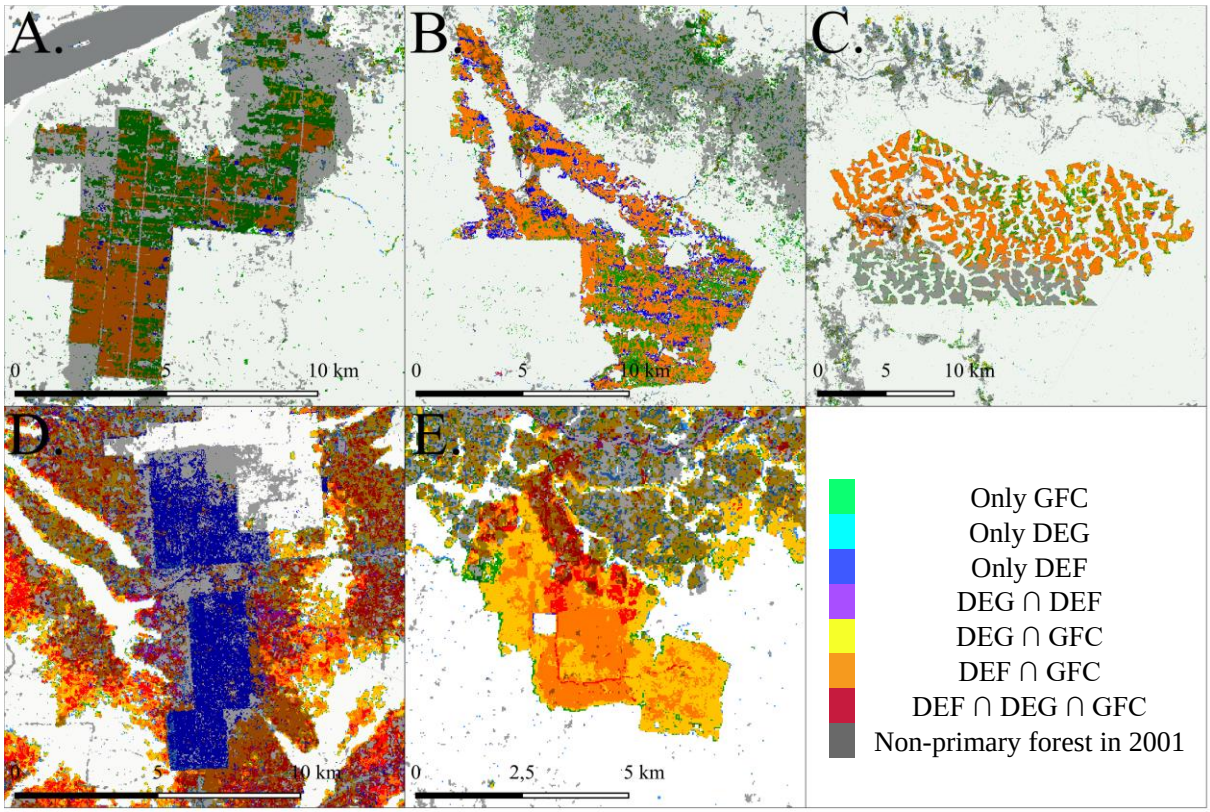

Figure 16: *Five industrial plantations.* ***A.*** *Old Gabonese palm oil plantation located near Makouké,* ***B.*** *new Olam oil palm plantation located near Kafele in Gabon,* ***C.*** *extension of old Olam rubber plantation near Okok in Gabon,* ***D.*** *old Unilever-founded (1944) plantation of Mokaria producing rubber and cocoa near Gwaka in DRC and* ***E.*** *young oil palm plantation (2016-2017) located near Tshakala in DRC. Shadowed detections are perturbations located in areas outside of the 2001 primary forest mask..*

3.7.3 Rural complex

The rural complex is by far the land use leading to most disturbance in the Central African moist forest. These mosaics of alternating cultivated plots, fallow land and old to recent forests regrowth form a multifaceted landscape in which the forests are often very degraded. Figure 17 shows the diversity of possible types of intersection within this complex. It can be seen that most of the current complex encircling the major towns in the Basin were already being farmed in 2001, even though large deforestation fronts can be seen at the edge of the complex.

Up to two-thirds of the detections are typically in landscapes already degraded in 2001 (located outside of the *2001 primary forest mask*). Using the GFC and TMF data to detect disturbances in these landscapes is a challenging exercise given the rural dynamics undergoing in the region, with alternating plots of farmland, slash-and-burn and fallow land. High-intensity disturbances can cause a change in land cover while there was no change in land use. This conflict between land use and land cover in terms of interpretation of GFC and TMF products inside the already existing rural complex must be addressed as it represents a significant fraction of the Congo Bassin Forest disturbances. In areas with high number of yearly available data, an intersection class gradient can be seen from the centre to the edges of the

complex. The DEG ∩ DEF ∩ GFC and DEG ∩ DEF classes can be found in the centre while GFC ∩ DEG and only DEG classes are more predominant at the front of the tropical moist forest. When it comes to the extension of this rural complex during the 21st century, GFC and TMF mostly agreed on both the location and the year of the perturbations. In area where data are scarce, mainly around the Gulf of Guinea, GFC, DEG ∩ GFC and only DEG intersection types make up most of the total detections. This fact further highlights that the distinction between a degraded forest and a deforested land in TMF product is not always a question of intensity or duration but instead a matter of data availability.

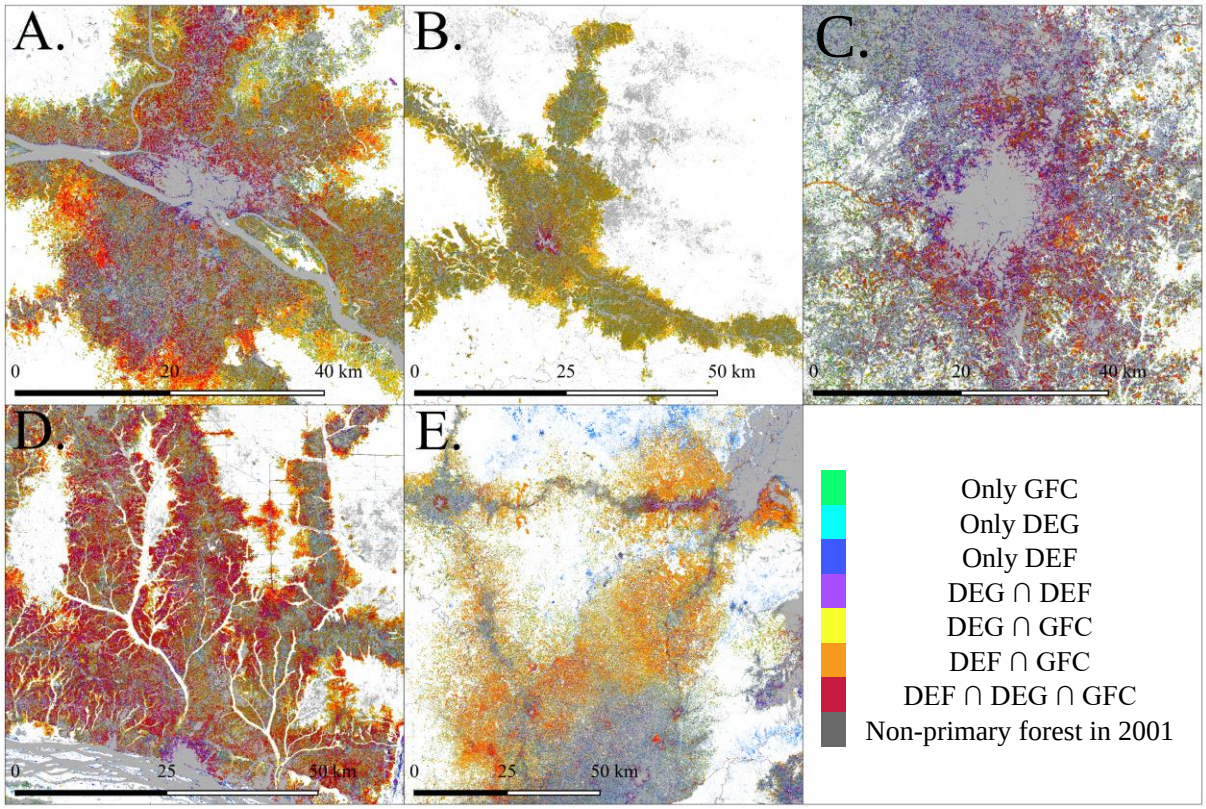

***Figure 17**: Five of the largest rural complex areas in the Congo Basin region surrounding **A.** Kisangani (DRC), **B.** Lubutu (DRC), **C.** Yaoundé (Cameroun), **D.** Bumba (DRC) and **E.** Bunia (DRC). The shadowed pixels are the perturbation located inside the 2001 already existing rural complex.*

3.7.4 Sparse riparian forests

At the south and north edges of the Congolese cuvette, the Kasaï, Ubangi and Mbomou river tributaries created an archipelago network of thin riparian forests. Those forests are located in densely populated areas and are subject to chronic degradation events. Those forests are semantically speaking at the edges of the dense tropical moist forest domain, as they are located far from the equatorial climatic zone and have low canopy height and canopy cover. In the intersection maps (Figure 18), those forest disturbance are covered by the DEG ∩ DEF, only DEG, and only DEF classes and principally entirely located within the non-primary forest domain. This further define the DEG ∩ DEF class as disturbance events located within already highly degraded forest extent. The lack of intersection between GFC and TMF in this landscape might be explained by the high seasonal effects and chronical degradation process inherent to this forest type, perturbating both TMF and GFC change detection algorithms. This induces to commission error for the former and omission errors for the latter.

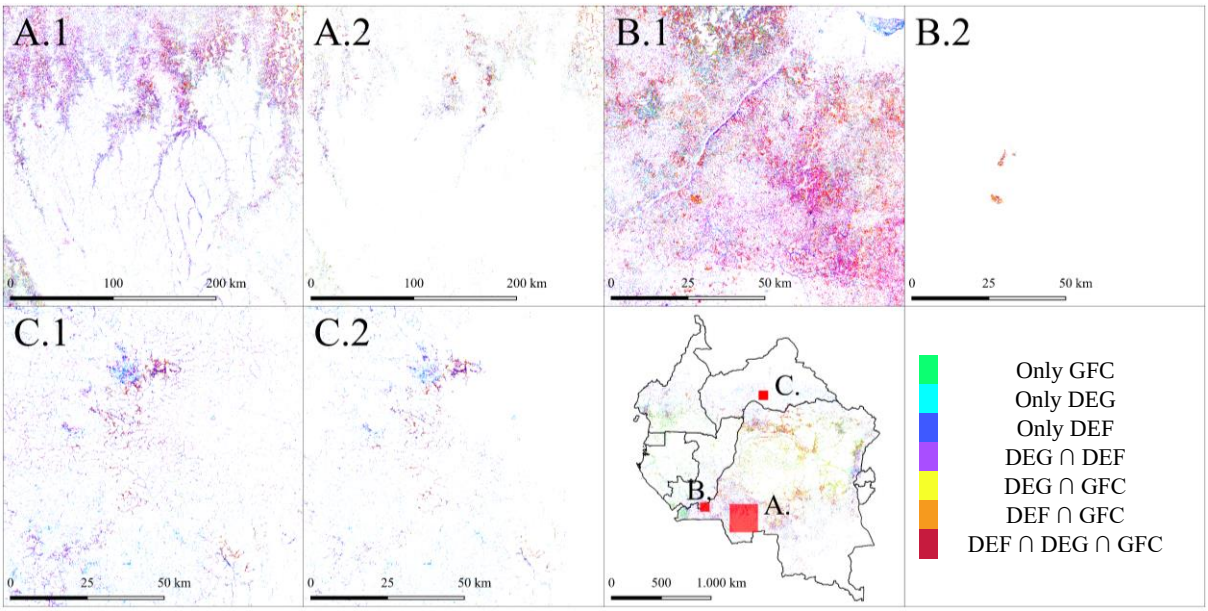

***Figure 18**: Intersection map zoom-in on the detections located within the riparian complex at north and south edges of the African rain forest. **1.** Detections inside the undisturbed forest and **2.** detections inside primary forest.*

3.7.5 Forest edges and algorithms sensibility

As shown in Figure 19, a non-negligible part of the divergences is found at the limit of the large convergence area. This halo of disturbance detected only by GFC or TMF is due to the sensitivity of their algorithm at the local level to pixels located between a disturbed and an undisturbed forest. These pioneering disturbances are not without interest because they reflect the reality of the damage caused by the opening of a canopy that was closed until then (windfall, drying out, ...). The category of perturbation also includes selective logging patches and temporary logging roads.

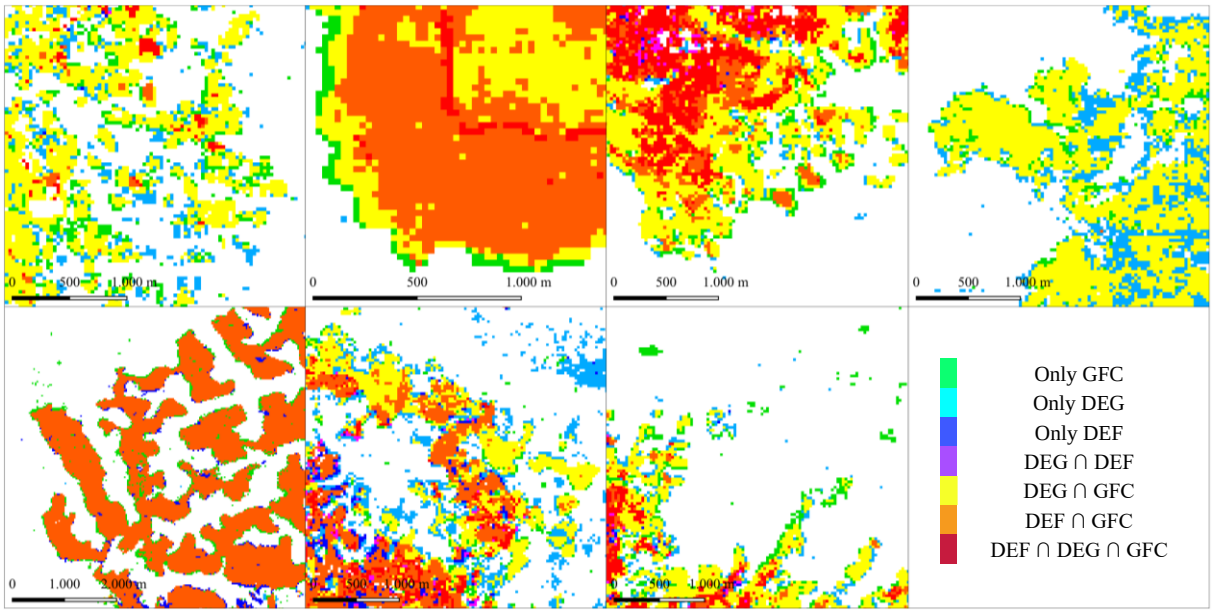

***Figure 19**: Various examples of divergences occurring at the edges of greater convergence areas.*

3.8 Conclusion

The review of the six currently operational forest monitoring systems described two long-term annual mapping systems using optical data and four SAR-based alert systems providing timely but much more conservative forest change detection (high omission errors). A pixel-level basin wide analysis of the two mapping systems highlight convergence in specific situations (59% for forest disturbance in the primary forest mask), but also major discrepancies all over the Congo Basin. The twenty-years long analysis also highlights some convergence trends of both systems, thanks to Landsat data quantity and quality, reaching today almost 50% of the total GFC and TMF detections.

The comparative analysis of GFC and TMF systems has made it possible to identify the different causes of their divergences and convergences for long term forest monitoring (2001-2021). In order to conclude this study, an adjusted definition of the GFC-TMF classes is provided to correspond mostly to each type of intersection and forest masks, based on empirical results and not just on methodological analysis of the respective systems. A recapitulative table on systems characteristics is available in *Appendix 7*. Here are the findings for each type of GFC-TMF intersection:

- **Only DEG:** Disturbance happening in all types of moist forest located at the edges of the 6 other classes mostly inside non primary forest extent. Can be located inside primary forest in cloudy area or in a selective logging context. Concentrate the large amount of false positive caused by clouds, seasonality and a TMF algorithm sensitivity. Due to data scarcity, spatial and temporal unevenness, a significant part of DEG detection could be associated with deforestation event and not degradation process.
- **Only DEF:** Intense perturbation happening in sparse relatively small moist forest located near rivers experiencing or old plantation usual clear cut. Focus on highly degraded forest.
- **Only GFC:** Intense recent or short-duration perturbation happening inside moist forest located mainly inside primary forest or at the edges of the rural complex. Most present in dense cloudy area.
- **DEG ∩ DEF:** Long term intense perturbation leading to permanent land cover change happening inside sparse forest located inside lightly degraded area near rivers and towns.
- **DEG ∩ GFC:** Main rural complex deforestation front, representing 1/3 of the primary forest loss. Progressively replacing DEF ∩ GFC label in the rural complex.
- **DEF ∩ GFC:** Long term conversion of moist forest into other land cover inside primary and non-primary area. Usually concerns new industrial plantations clear cutting, intense perturbation located at the edges of the rural complex and permanent conversion into other commodities.
- **DEF ∩ DEG ∩ GFC:** Long term intense perturbation leading to permanent land cover change happening inside moist forest located inside lightly degraded area near rivers and towns experiencing.

GFC detections are mostly located inside closed canopy forests and so do not detect changes in sparse forests or forests subject to chronic degradation processes. TMF detections are located in all forest canopies within the dense and humid zone, even in open and highly degraded canopies. The TMF product is extremely sensitive to variations in edaphic conditions that modify canopy structure, whereas GFC tends to ignore them as long as they do not lead to a total loss of forest cover.

These definitions provide a general framework for each of the definitions. The different systems and their intersections are often part of complex spatial and temporal dynamics, so that the analysis of their intersections alone is not enough to completely define the nature of their detections. Still, this first complementary study highlights the spatial, temporal, semantic and thematic of both global datasets,

advocating for a consolidation aligned with the specific needs of the COMIFAC countries for the tropical moist forest reliable monitoring.

Appendix

Appendix 1: *Table containing the proportion of CAFI samples well classified by land cover for GLAD and JRC TMF mask. The third column displayed the overall agreement between GLAD and JRC mask by Land Cover. The last column shows the number of samples for each land cover.*

		GLAD primary TMF mask	JRC primary TMF mask	Overall agreement	Samples
Non TMF	Forêts secondaires	0,77	0,69	0,88	16752
	Plantations forestières	0,75	0,75	0,75	8
	Forêts dense sêches	0,95	0,94	0,97	8651
	Forêts claires sèches	0,97	0,96	0,98	26900
	Savanes arborées	0,96	0,96	0,98	13224
	Savanes arbustives	0,92	0,90	0,96	8651
	Prairies aquatiques	0,92	0,89	0,95	35883
	Savanes herbacées	0,96	0,95	0,98	29295
	Terres cultivées	0,90	0,86	0,93	6057
	Sols nus	0,95	0,93	0,97	20749
	Terres bâties	0,76	0,68	0,90	26900
	Eau	0,76	0,73	0,95	4198
TMF	Forêts denses	0,78	0,84	0,91	157615
	Forêts galeries	0,08	0,10	0,95	4687
	Forêts marécageuses	0,74	0,76	0,96	15836
	Mangroves	0,48	0,79	0,67	311
	Forêts montagnardes	0,45	0,54	0,83	750
	Forêts sub-montagnardes	0,58	0,66	0,89	3377

Appendix 2: *Proportion of each intersection classes for all COMIFAC countries containing tropical moist forest between 2001 and 2021 within primary, undisturbed, and non-primary tropical moist forest masks*

A. Primary Forest mask

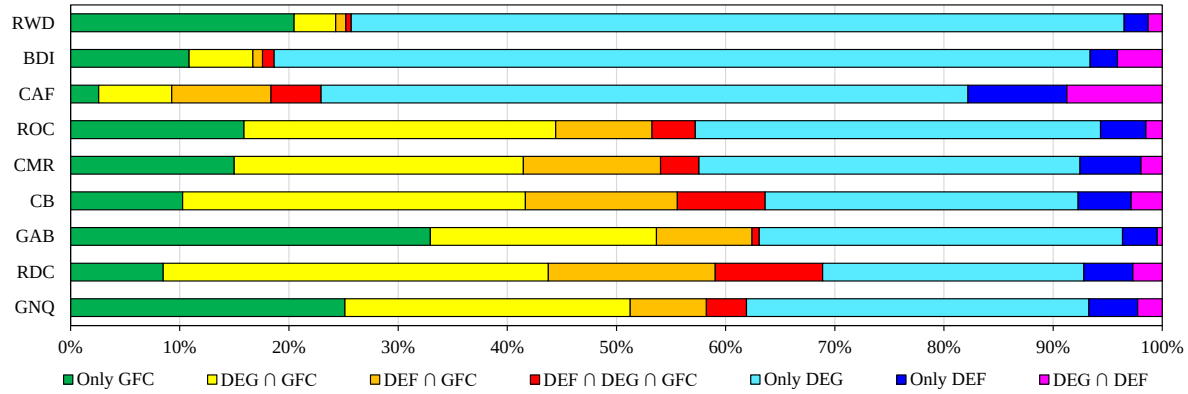

B. Undisturbed tropical moist forest mask

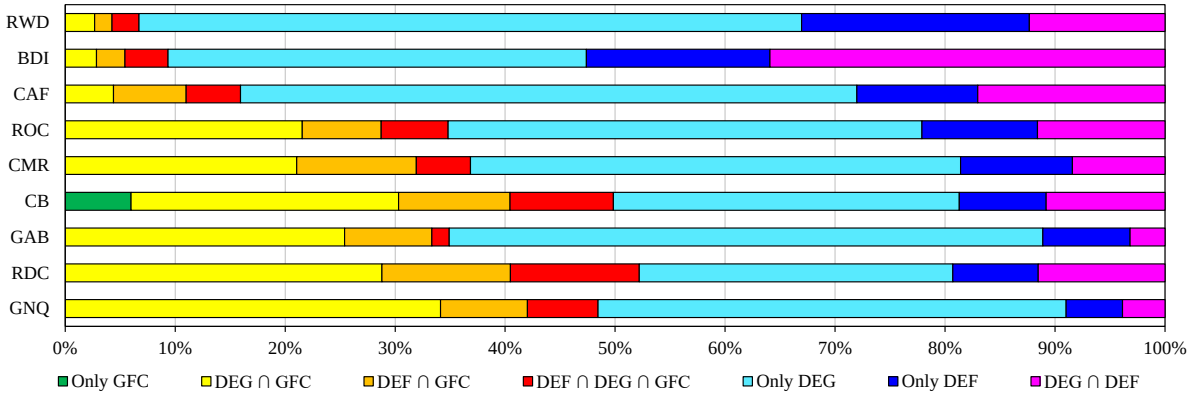

C. Non Primary Forest mask

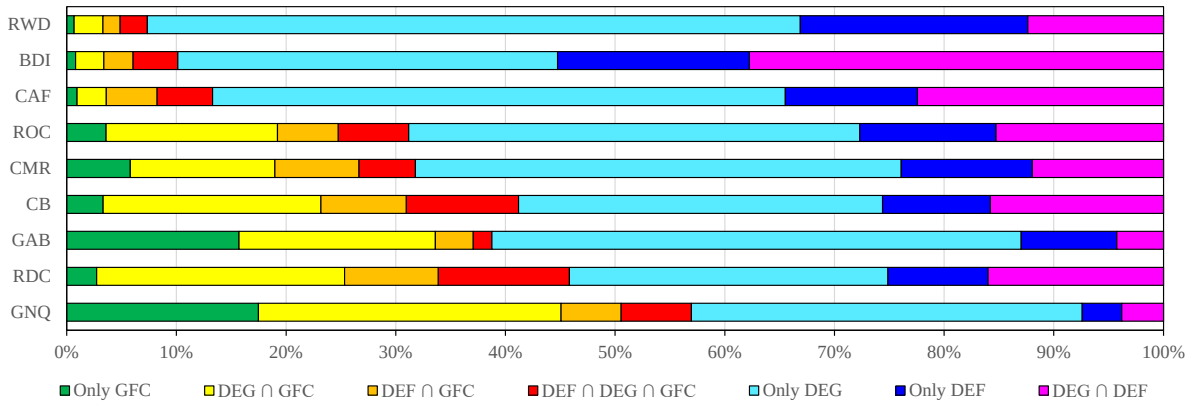

Appendix 3: *Cumulative and disaggregated distribution of intersection types according to the percentage of tree cover in 2000 for all disturbances detected between 2001 and 2021 within primary tropical moist forest masks.*

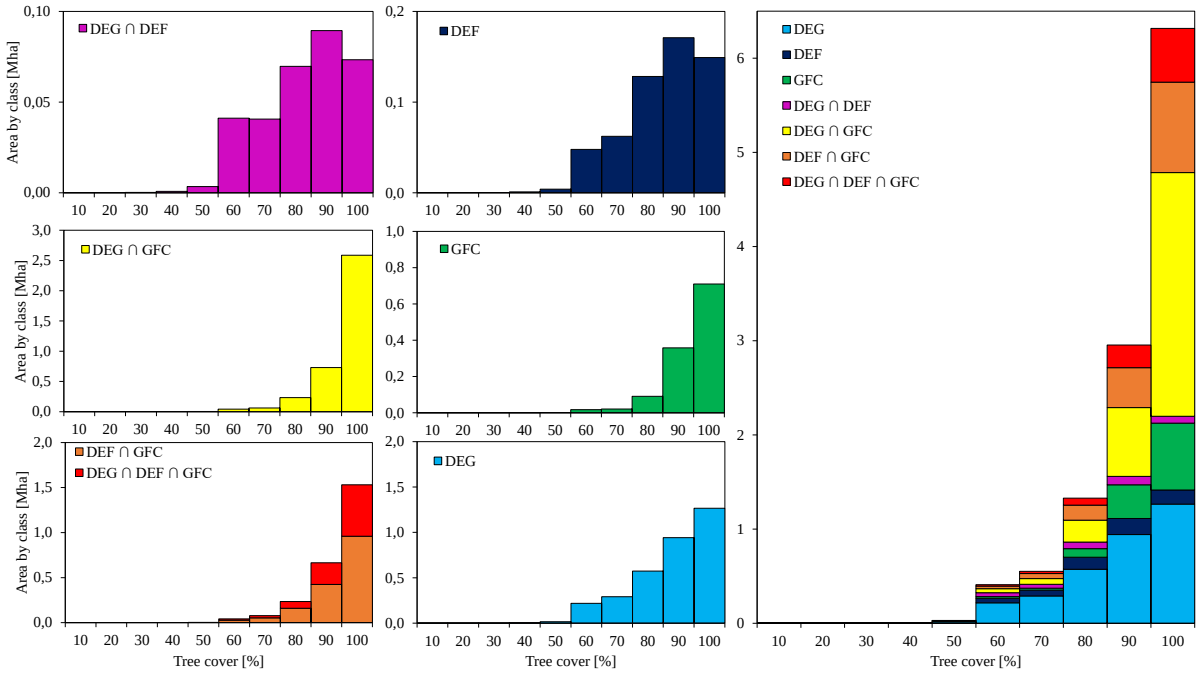

Appendix 4: *Cumulative and disaggregated distribution of intersection types according to the percentage of tree cover in 2000 for all disturbances detected between 2001 and 2021 within non-primary tropical moist forest.*

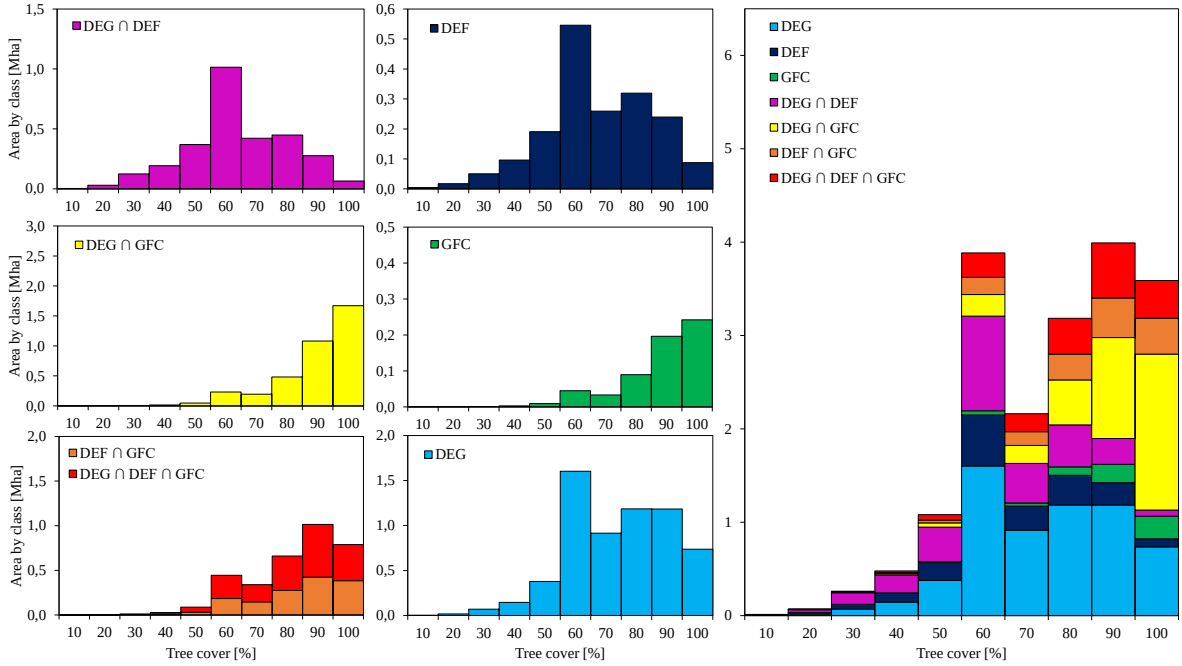

Appendix 5: *Intersection maps for each COMIFAC countries for A) Undisturbed B) Primary Forest masks.*

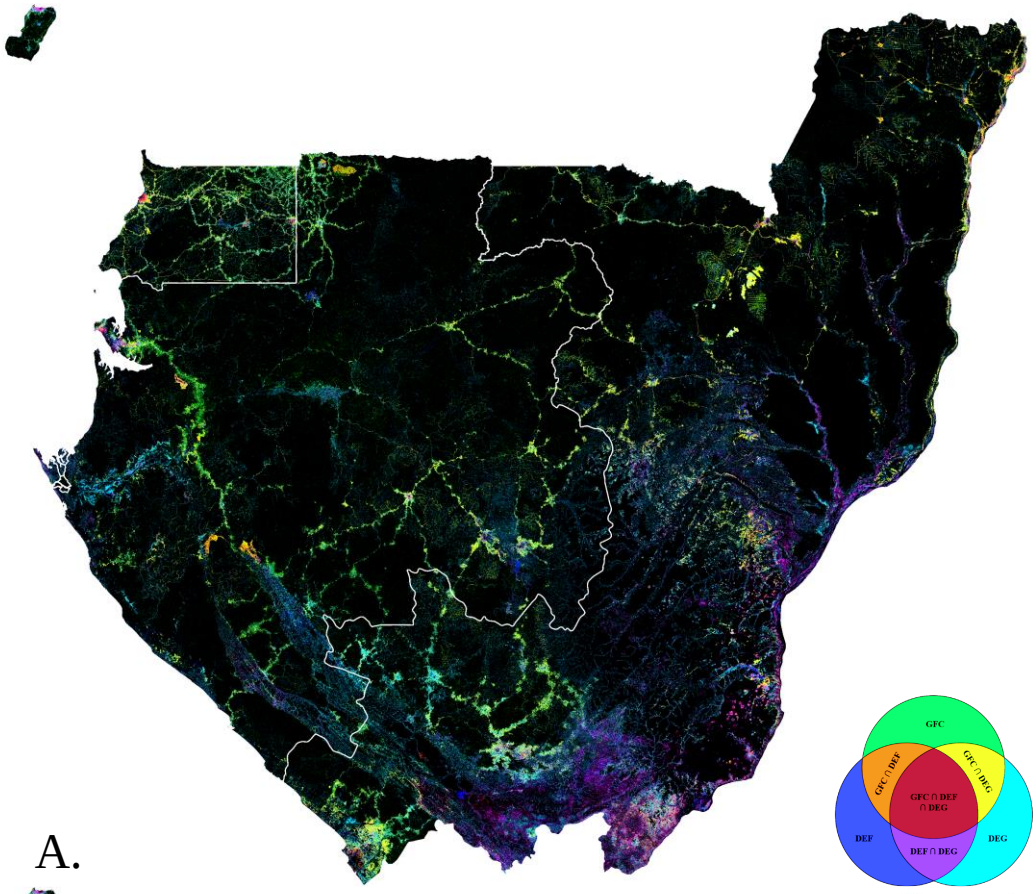

A.

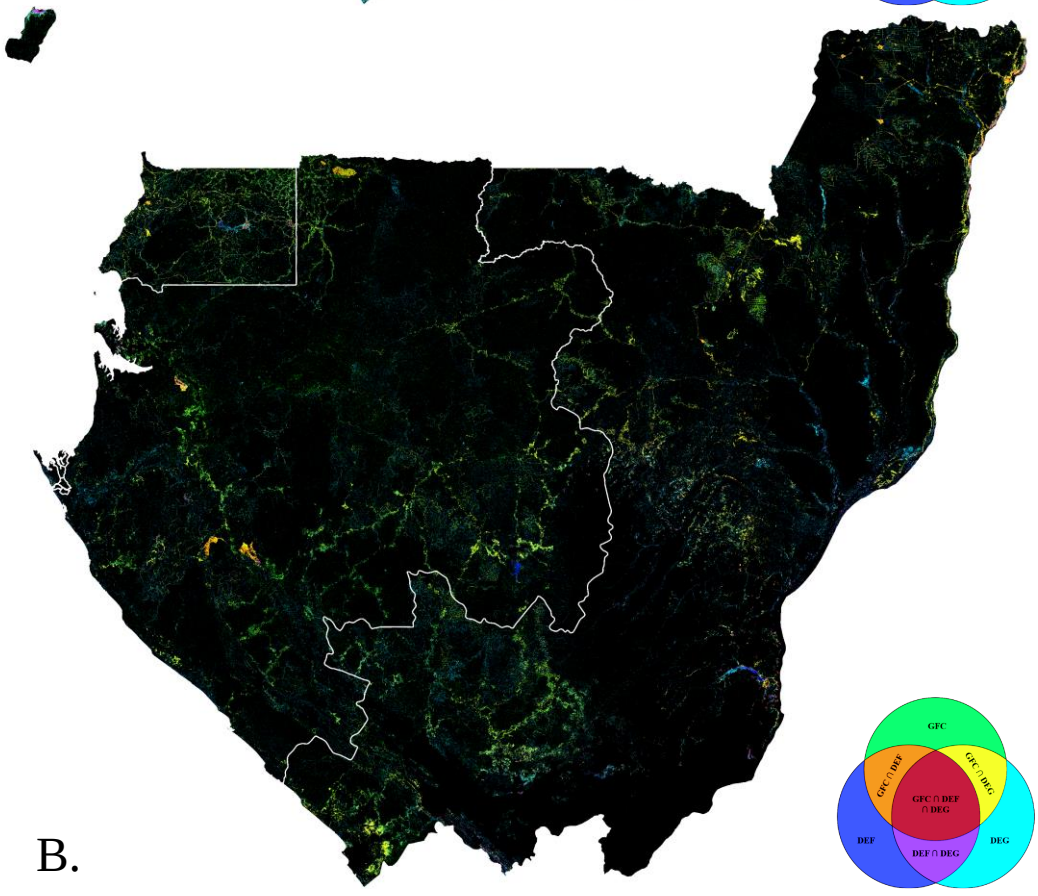

B.

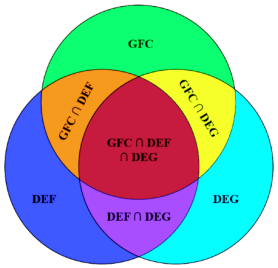

A.

B.


GFC
GFC ∩ DEF
GFC ∩ DEG
GFC ∩ DEF
∩ DEG
DEF
DEG
DEF ∩ DEG

A.


GFC
GFC ∩ DEF
GFC ∩ DEG
GFC ∩ DEF
∩ DEG
DEF
DEG
DEF ∩ DEG

B.

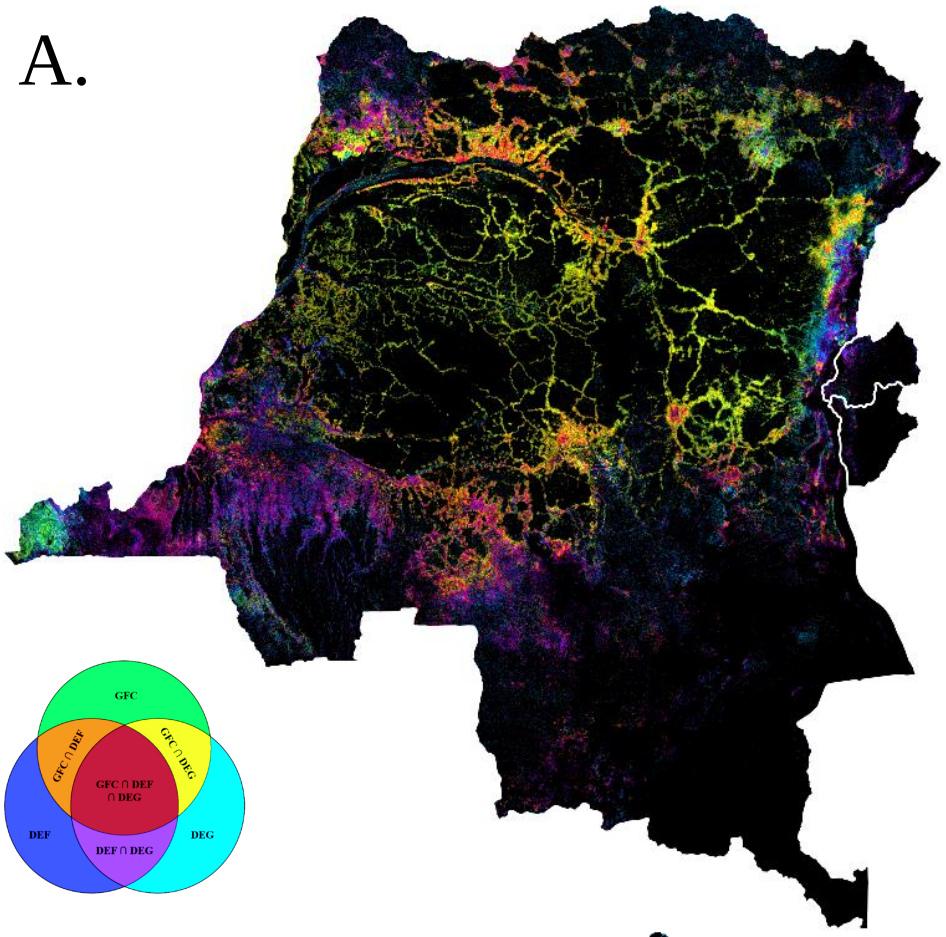
A.
GFC
GFC ∩ DEF
GFC ∩ DEG
GFC ∩ DEF ∩ DEG
DEF
DEG
DEF ∩ DEG

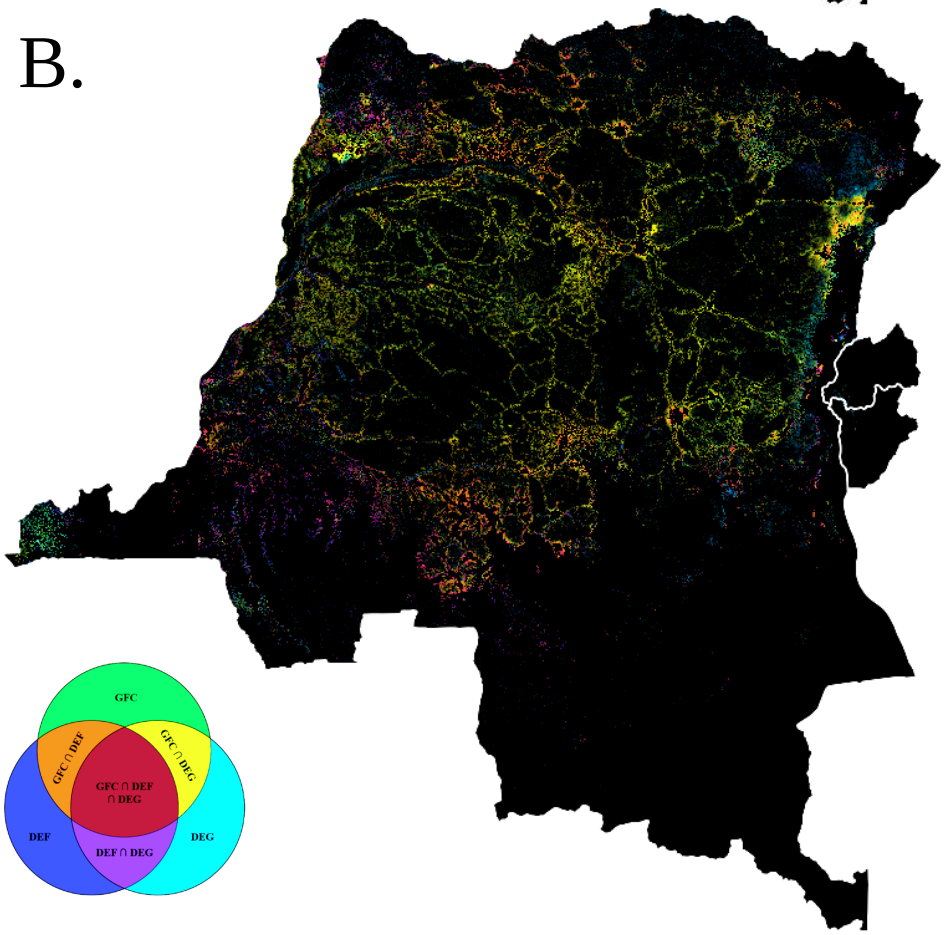
B.
GFC
GFC ∩ DEF
GFC ∩ DEG
GFC ∩ DEF ∩ DEG
DEF
DEG
DEF ∩ DEG

Appendix 6: *Intersection statistics for each COMIFAC countries for undisturbed and primary forest masks.*

Central African Republic						
Intersection class	Undisturbed Mha			Primary Mha		
Only GFC	0,03	0,03		0,02	0,02	
Only DEG	1,02			0,45		
Only DEF	0,20	1,54		0,07	0,59	
DEG ∩ DEF	0,31		1,85	0,07		0,77
DEG ∩ GFC	0,08			0,05		
DEF ∩ GFC	0,12	0,28		0,07	0,16	
DEF ∩ DEG ∩ GFC	0,09			0,04		

Democratic Republic of the Congo						
Intersection class	Undisturbed Mha			Primary Mha		
Only GFC	1,09	1,09		0,71	0,71	
Only DEG	6,03			2,01		
Only DEF	1,64	10,11		0,38	2,61	
DEG ∩ DEF	2,44		22,23	0,23		8,40
DEG ∩ GFC	6,09			2,96		
DEF ∩ GFC	2,47	11,04		1,29	5,07	
DEF ∩ DEG ∩ GFC	2,48			0,83		

Republic of the Congo						
Intersection class	Undisturbed Mha			Primary Mha		
Only GFC	0,15	0,15		0,10	0,10	
Only DEG	0,78			0,19		
Only DEF	0,19	1,18		0,06	0,28	
DEG ∩ DEF	0,21		1,96	0,03		0,65
DEG ∩ GFC	0,39			0,24		
DEF ∩ GFC	0,13	0,62		0,03	0,27	
DEF ∩ DEG ∩ GFC	0,11			0,01		

Republic of Cameroun						
Intersection class	Undisturbed Mha			Primary Mha		
Only GFC				0,21	0,21	
Only DEG	1,27			0,48		
Only DEF	0,29	1,80		0,08	0,59	
DEG ∩ DEF	0,24		3,16	0,03		1,38
DEG ∩ GFC	0,60			0,37		
DEF ∩ GFC	0,31	1,05		0,17	0,59	
DEF ∩ DEG ∩ GFC	0,14			0,05		

Republic of Gabon						
Intersection class	Undisturbed Mha			Primary Mha		
Only GFC	0,20	0,20		0,13	0,13	
Only DEG	0,34			0,13		
Only DEF	0,05	0,41		0,01	0,15	
DEG ∩ DEF	0,02		0,84	0,00		0,40
DEG ∩ GFC	0,16			0,08		
DEF ∩ GFC	0,05	0,23		0,04	0,12	
DEF ∩ DEG ∩ GFC	0,01			0,00		

Equatorial Guinea						
Intersection class	Undisturbed Mha			Primary Mha		
Only GFC	0,04	0,04		0,03	0,03	
Only DEG	0,06			0,03		
Only DEF	0,00	0,08		0,00	0,04	
DEG ∩ DEF	0,02		0,21	0,00		0,10
DEG ∩ GFC	0,06			0,03		
DEF ∩ GFC	0,00	0,08		0,01	0,04	
DEF ∩ DEG ∩ GFC	0,02			0,00		

Republic of Rwanda						
Intersection class	Undisturbed Mha			Primary Mha		
Only GFC	0,03	0,03		0,00		
Only DEG	0,03			0,00		
Only DEF	0,02	0,08		0,00	0,00	
DEG ∩ DEF	0,04		0,09	0,00		0,00
DEG ∩ GFC	0,00			0,00		
DEF ∩ GFC	0,00	0,01		0,00	0,00	
DEF ∩ DEG ∩ GFC	0,00			0,00		

Republic of Burundi						
Intersection class	Undisturbed Mha			Primary Mha		
Only GFC	0,00	0,00		0,00		
Only DEG	0,01			0,00		
Only DEF	0,00	0,02		0,00	0,00	
DEG ∩ DEF	0,01		0,02	0,00		0,00
DEG ∩ GFC	0,00			0,00		
DEF ∩ GFC	0,00	0,00		0,00	0,00	
DEF ∩ DEG ∩ GFC	0,00			0,00		

Appendix 7: *Recapitulative tables on systems characteristics. The first table shows the percent tree cover and forest height for the seven intersection classes. The second table shows a qualitative description of those classes in regards with the main landscapes in which they occurred and a short definition.*

	Proportion in Primary forest [%]	Average % tree cover Undisturbed forest	Average % tree cover Primary forest	Average % tree cover Non-primary forest	2020-2019 tree height [m]	2001-2018 tree height [m]
Only GFC	66	92,20	94,27	88,19	23,43	13,05
Only DEG	35	78,99	88,11	74,15	19,24	12,13
Only DEF	24	71,62	85,15	67,41	13,56	8,35
DEG ∩ DEF	10	65,78	83,08	63,91	-	-
DEG ∩ GFC	50	92,57	95,71	89,49	23,25	11,91
DEF ∩ GFC	53	88,89	93,68	83,56	22,37	7,62
DEF ∩ DEG ∩ GFC	37	85,98	94,30	81,96	-	-

Intersection classes	Main detction landscapes	Derived definition for each intersection type
Only DEF	Riparian archipelago Flooded forest Riverside Dams river bed Old plantation	Sparse relatively small moist forest located near rivers experiencing intense perturbation or old plantation usual clear cut. Focus on highly degaded forest.
DEG ∩ DEF	Riparian archipelago Riverside Rural complex -center-	Sparse moist forest located inside higly degraded area near rivers & towns experiencing long term intense perturbation
DEF ∩ DEG ∩ GFC	Rural complex -center-	Moist forest located inside lightly degraded area near rivers & towns experiencing long term intense perturbation leading to permanent land cover change.
Only GFC	Primary forest New plantations Deforestation front interface with primary forest Rural complex -edges-	Moist forest located mainly inside primary forest or at the edges of the rural complex experiencing intense recent or short perturbation. Most present in dense cloudy area.
DEF ∩ GFC	New plantations Primary forest Rural complex -edges-	Long term conersion of moist forest into other land cover inside primary & non-primary area. Usualy conerns new industrial plantations clear cuting & intense perturbation located at the edges of the rural complex.
DEG ∩ GFC	Primary forest Rural complex -edges-	Main ural complex deforestaion front, representing 1/3 of the primary forest loss
Only DEG	Flooded forest Riparian archipelago Rural complex -center- Primary forest Deforestation front interface with primary forest Rural complex -edges-	Usualy located at the edges of the 6 other classes mostly inside non primary forest extent. Located inside primary forest t in dense cloudy area or in a selective logging context. Concentrate the large amount of false positive caused by clouds, seasonality & aTMF algorithm sensitivity.

References

Dalimier J. et al., "***Characterizing the Congo Basin Forests by a Detailed Forest Typology Enriched with Forest Biophysical Variables***," 2021 IEEE International Geoscience and Remote Sensing Symposium IGARSS, Brussels, Belgium, 2021, pp. 673-676, doi: 10.1109/IGARSS47720.2021.9553905

Lamarche, C., Bontemps, S., Rousseau, C., De Maet, T., Verhegghen, A., Radoux, J., Van Bogaert, E., Arino, O. and Defourny, P., 2014. " CCI-LC seasonality product. Characterizing the reference dynamics of the land surface. In The 4th International Symposium on Recent Advances in Quantitative Remote Sensing: RAQRS'IV.

Gou Y. et al (2022) ***Intra-annual relationship between precipitation and forest disturbance in the African rainforest***. Environ. Res. Lett. 17 044044 doi:10.1088/1748-9326/ac5ca0

Potapov P., X. Li, A. Hernandez-Serna, A. Tyukavina, M.C. Hansen, A. Kommareddy, A. Pickens, S. Turubanova, H. Tang, C.E. Silva, J. Armston, R. Dubayah, J. B. Blair, M. Hofton (2020) ***Mapping and monitoring***

global forest canopy height through integration of GEDI and Landsat data. Remote Sensing of Environment, 112165. https://doi.org/10.1016/j.rse.2020.112165

Turubanova S., Potapov P., Tyukavina, A., and Hansen M. (2018) ***Ongoing primary forest loss in Brazil, Democratic Republic of the Congo, and Indonesia***. Environmental Research Letters https://doi.org/10.1088/1748-9326/aacd1c

Tyukavina A. et al., (2018) ***Congo Basin Forest loss dominated by increasing smallholder clearing***. Sci. Adv.4, eaat2993. DOI:10.1126/sciadv.aat2993

USGS (2020) ***Fifty years of Landsat: Sharing Earth information for the benefit of all***. https://www.usgs.gov/news/featured-story/fifty-years-landsat-sharing-earth-information-benefit-all

World Agroforestry (2018) ***Musanga cecropioides*** https://apps.worldagroforestry.org/treedb2/AFTPDFS/Musanga_cecropioides.PDF